Titre: Title:	Preliminary Assessment of the Vibro-Peening Process for Improving the Fatigue Life of Aerospace Components
Auteur: Author:	Léo Canals
Date:	2018
Type:	Mémoire ou thèse / Dissertation or Thesis
Référence: Citation:	Canals, L. (2018). Preliminary Assessment of the Vibro-Peening Process for Improving the Fatigue Life of Aerospace Components [Mémoire de maîtrise, École Polytechnique de Montréal]. PolyPublie. https://publications.polymtl.ca/3009/

URL de PolyPublie: PolyPublie URL:	https://publications.polymtl.ca/3009/
Directeurs de recherche: Advisors:	Martin Lévesque
Programme: Program:	Génie mécanique

UNIVERSITÉ DE MONTRÉAL

PRELIMINARY ASSESSMENT OF THE VIBRO-PEENING PROCESS FOR
IMPROVING THE FATIGUE LIFE OF AEROSPACE COMPONENTS

LÉO CANALS
DÉPARTEMENT DE GÉNIE MÉCANIQUE
ÉCOLE POLYTECHNIQUE DE MONTRÉAL

MÉMOIRE PRÉSENTÉ EN VUE DE L'OBTENTION
DU DIPLÔME DE MAÎTRISE ÈS SCIENCES APPLIQUÉES
(GÉNIE MÉCANIQUE)
MARS 2018

UNIVERSITÉ DE MONTRÉAL

ÉCOLE POLYTECHNIQUE DE MONTRÉAL

Ce mémoire intitulé :

PRELIMINARY ASSESSMENT OF THE VIBRO-PEENING PROCESS FOR
IMPROVING THE FATIGUE LIFE OF AEROSPACE COMPONENTS

présenté par : CANALS Léo
en vue de l'obtention du diplôme de : Maîtrise ès sciences appliquées
a été dûment accepté par le jury d'examen constitué de :

M. TURENNE Sylvain, Ph. D., président
M. LÉVESQUE Martin, Ph. D., membre et directeur de recherche
M. MARTINU Ludvik, Ph. D., membre

DEDICATION

À Nicole et Bernard,
À Passipierre et Maminette,
À mes parents....

ACKNOWLEDGMENTS

RÉSUMÉ

Le vibro-grenaillage est un procédé dérivé du vibro-finissage qui a pour double objectif la finition de pièces métalliques et l'introduction de contraintes résiduelles compressives pour l'amélioration de la vie en fatigue. Bien que ce procédé apparaisse dans la littérature depuis les années 2000, très peu d'articles ont été publiés sur le sujet.

Cette étude, réalisée en partenariat avec Safran Aerospace Defense Security et VibraFinish Ltd, a pour objectif de quantifier les effets du vibro-grenaillage sur des alliages utilisés dans l'industrie aérospatiale afin d'en évaluer le potentiel pour des applications industrielles. Cette étude expose les effets du vibro-grenaillage sur l'alliage titane Ti-6Al-4V et l'alliage d'acier cémenté E-16NiCrMo-13, dont les échantillons ont été fournis par Safran, et les compare à ceux induits par le grenaillage traditionnel, utilisant comme paramètre de contrôle l'intensité Almen. Les effets mesurés dans cette étude sont la rugosité de surface, les contraintes résiduelles en compression ainsi que la dureté. La revue de littérature a montré que la fréquence et la masse de média étaient potentiellement significatifs sur les effets induits par le procédé. Ces paramètres ont été retenus comme variables pour l'étude. L'étude présentée démontre la capacité du procédé de vibro-grenaillage à atteindre des intensités Almen comparables à celles atteintes par le procédé de grenaillage dans l'industrie aérospatiale, les intensités ciblés étant 0.12 mmA, 0.18 mmA et 0.25 mmA. Les échantillons d'alliage titane et acier ont finalement été traités à ces trois intensités puis observés en termes de rugosité, dureté et contraintes résiduelles. Finalement, des échantillons des mêmes matériaux ont été grenaillés aux intensités 0.12 mmA et 0.18 mmA dans les laboratoires de Safran, nous permettant une comparaison fidèle des deux procédés.

Cette étude démontre que le vibro-grenaillage est capable de produire systématiquement des intensités de grenaillage entre 0.12 mmA et 0.25 mmA. De plus, il a été montré que le procédé induisait des contraintes résiduelles en compression et modifiait l'aspect de surface des pièces, réduisant (E-16NiCrMo13) ou effaçant (Ti-6Al-4V) les marques de fraisage et de rectifiage des échantillons. La rugosité moyenne de surface a été abaissée à 0.3-0.4 μm pour les deux matériaux. Cette étude permet également de conclure que la dureté en surface des échantillons a été accrue par le vibro-grenaillage, indépendamment des paramètres machine. À intensités Almen égales, le vibro-grenaillage a induit des contraintes en compression plus importantes et plus profondes que le grenaillage traditionnel. Également, le vibro-grenaillage a produit une rugosité plus faible que le grenaillage traditionnel. Le potentiel du procédé de vibro-grenaillage à combiner deux procédés en un (finition et grenaillage) ou éventuellement augmenter la vie en fatigue, a été démontré.

ABSTRACT

Vibratory peening derives from vibratory finishing and aims to induce beneficial compressive residual stresses while simultaneously polishing the treated part. Even though this process appeared in literature since the 2000s, only a few public articles have been published on this topic.

This study, realized in partnership with Safran Aerospace Defense and Security and VibraFinish Ltd, investigates the vibratory peening effects, in terms of residual stresses, roughness and hardening, on aerospace alloys. The investigation focused on titanium alloy Ti-6Al-4V and case hardened steel E-16NiCrMo13 samples provided by Safran. The effects induced by the vibratory peening process have been compared to the effects induced by the shot peening process, using Almen intensity as a control parameter. The measured effects were surface roughness, sub-surface compressive residual stresses fields and hardness profiles.

The literature review identifies the tub vibration frequency and the mass of media as influential machine parameters on the vibratory peening effects. The influence of these parameters is investigated in the study. The experimental results presented next demonstrate the capacity of the vibratory peening process to reach Almen intensities ranging from 0.12 mmA to 0.25 mmA, which is comparable to the shot peening intensities used in the aerospace industry. Titanium and steel samples have been vibratory peened at 0.12 mmA, 0.18 mmA and 0.25 mmA and resulting roughness, residual stresses and hardness have been measured. Samples from the same materials have been shot peened at 0.12 mmA and 0.18 mmA at Safran Tech laboratories to compare the effects of both processes.

The main conclusions of that study are that vibratory peening can consistently deliver peening intensity in the range of 0.12 mmA - 0.25 mmA. Furthermore, it has been shown that the process induced a compressive residual stress field and could modify the surface aspect of the parts, reducing (on E-16NiCrMo13) or erasing (on Ti-6Al-4V) milling marks. The surface roughness has been lowered down to 0.3-0.4 μm for both materials. The surface hardness has increased due to the vibratory peening process, independently of machine parameters. For similar Almen intensities, vibratory peening induced higher and deeper compressive residual stresses, when compared to those resulting from shot peening. Moreover, the vibratory peening process produced a lower surface roughness than the shot peening process. The study has demonstrated that vibratory peening could potentially combine fatigue life enhancement and surface finishing into a single processing step, and could even deliver higher fatigue lives than shot peening.

TABLE OF CONTENTS

LIST OF TABLES

LIST OF FIGURES

LIST OF ABBREVIATIONS

SP   Shot Peening

VP   Vibratory Peening

VF   Vibratory Finishing

VD   Vibratory Deburring

HCF   High Cycle Fatigue

LIST OF APPENDICES

CHAPTER 1 INTRODUCTION

Conventional shot peening is a well-known surface treatment used to enhance the fatigue life of metallic parts. The process consists in impacting a metal part with high velocity spherical shots. The impacts plastically deform and strech the surface, which induces a layer of compressive residual stresses and cold working. Shot peening retards the initiation and propagation of cracks, and hence increases fatigue life. This beneficial effect is counterbalanced by the increase of roughness that creates stress concentrators, which is detrimental to fatigue life. A surface finishing processing step is often required after shot peening to improve the resulting poor surface finish by smoothing it [1].

Vibratory finishing is a widely deployed process developed in the 1950s for polishing and deburring parts [2]. The process is applied with a container filled with polishing media in which the treated part is inserted. A vibrating system creates a periodic motion that shakes parts and media. The media mechanically polishes the parts' surface and improves its surface finish.

Vibratory peening is a vibratory finishing process in which the parts are fixed in the tub. When compared to vibratory finishing, having the part fixed in the tub increases the media impacting velocity, leading to higher energy transmitted to the part's surface. The process induces compressive residual stresses and work hardening on the near surface layer similar to those resulting from the shot peening process, without damaging the surface quality (production of a rough surface). The process combines the beneficial effects of both shot peening and vibratory finishing processes. Furthermore, vibratory peening can be more suitable for complex parts than shot peening, as demonstrated by Feldmann et al. for full blisk-rotors [3].

The purpose of this study was to assess the vibratory peening process potential to either replace or improve on the conventional shot peening process. This research is therefore essential to confirm the process' potential and lay the bases for forthcoming studies that would be aimed to thoroughly investigate its effects on target materials.

This research was done in collaboration with Safran Aerospace Security and Defense and VibraFinish Ltd. Safran is a French group, worldwide supplier for the aerospace industry, they provided the Ti-6Al-4V and E-16NiCrMo13 samples studied in this project. VibraFinish Ltd is a Canadian SME based in Mississauga and specialized in vibratory finishing, shot blasting and other finishing processes. They committed their experience and their own vibratory peening machine to this research. The rest of the funding was provided by the

National Sciences and Engineering Research Council (project CRDPJ 518968 - 17).

The thesis is divided in 5 chapters. Chapter 2 is an overview of the public literature covering the vibratory peening process. Chapter 3 presents the scientific objectives pertaining to this work and identified from the literature survey. Chapter 4 is an article submitted to the *Journal of Materials on Processing Technologies* and gathers the experimental work and results. A general discussion and a general conclusion are presented respectively in Chapters 5 and 6. Appendix A presents the measurements methods for the results presented in Chapter 4.

CHAPTER 2   LITERATURE REVIEW

2.1   Conventional shot peening

2.1.1   Process presentation

Shot Peening (SP) is a cold-working process that consists in projecting shots onto a metallic part, at high velocities. The shots impacting the surface transmit energy that produces plastic deformation. This deformation streches a surface layer about few hundreds of microns thick. As the core of the material is not deformed, a residual stress field is induced in the material, leading to compressive residual stresses in the sub-surface layer and tensile residual stresses in the core. The compressive stresses act as closure stresses that delay crack initiation and propagation [4]. The SP process also creates work hardening that induces a resistance to plastic deformation and specifically around the crack tip. However, the SP process induces roughness which has a detrimental effect on fatigue life [5]. The enhancement of fatigue life with shot peening is therefore a balance between favorable and detrimental effects. The use of optimal conditions can improves fatigue lives up to 50 times [6], when compared to as-machined parts, or yields endurance fatigue limits 80% higher [7].

2.1.2   Control parameters

Shot peening relies on two process control parameters: Almen intensity and coverage. Almen intensity is a standard testing procedure and consists in shot peening small strips of SAE 1070 steel, for different processing times. The strips are peened in a standardized fixture (Figure 2.1a) and their deflection is measured once they are taken out of the fixture with a standardized Almen gauge (Figure 2.1b). The procedure is repeated for different processing times and the arc height as a function of peening time is plotted as a saturation curve (Figure 2.1c). As described in standard SAE J443 [8], at least four points are needed to obtain the saturation curve. The saturation time is defined as the specific time after which doubling the peening time increases the arc height by 10%. The Almen intensity is the arc height at the saturation time.

The Almen intensity is measured with three different types of strips, namely N, A and C. These strips vary in thickness and are depicted in Figure 2.2. The change in strips's thickness allows a larger range of measurable Almen intensities. The Almen intensity measured on A-type strips is described by the mmA unit. Almen intensity is specified with these strips and

depends on the target application.

Coverage of a shot peened surface is defined by SAE J2277 [10] as the ratio (in percentage) of the surface indented by the shots to the total surface. Coverage is determined visually by an experimented eye or by computer assisted image analysis. Full coverage is set at 98%. Coverage values above 100% are multiples of the peening time required to reach 98% coverage.

2.1.3 Typical surface roughness and residual stresses induced by shot peening

Liu et al. [11] treated Ti-6Al-4V specimens at different intensities and 100% coverage. Figure 2.3a shows the resulting average roughness for different peening treatments. Xie et al. [12] peened Ti-6Al-4V samples at 0.20 mmA and 100% coverage. It can be observed that the
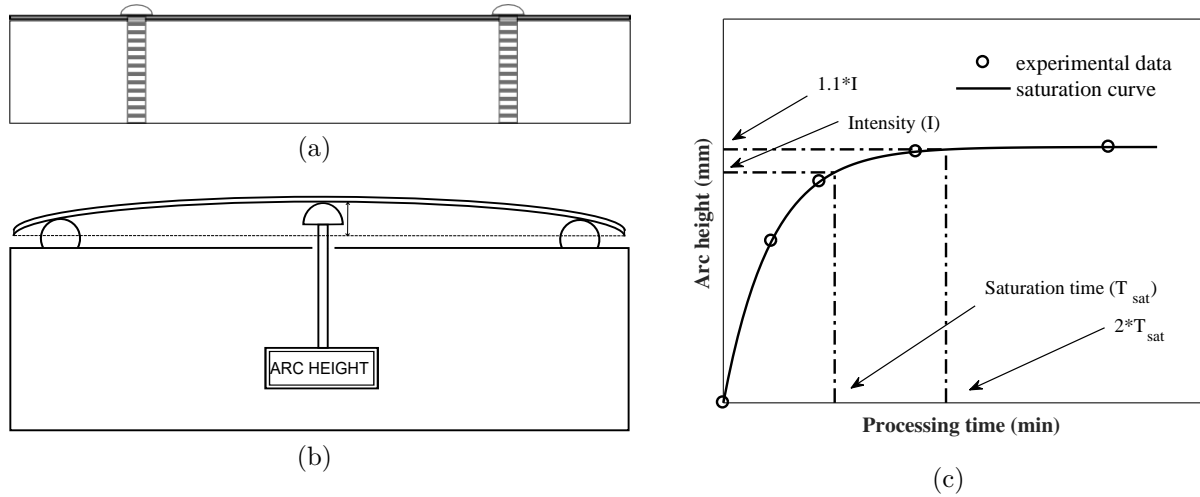
Figure 2.1 a) Flat strip on its holder, side view. b) Strips on the Almen gauge, measurement of arc height, side view. c) Saturation curve and Almen intensity calculation, as per SAE J443 [8]
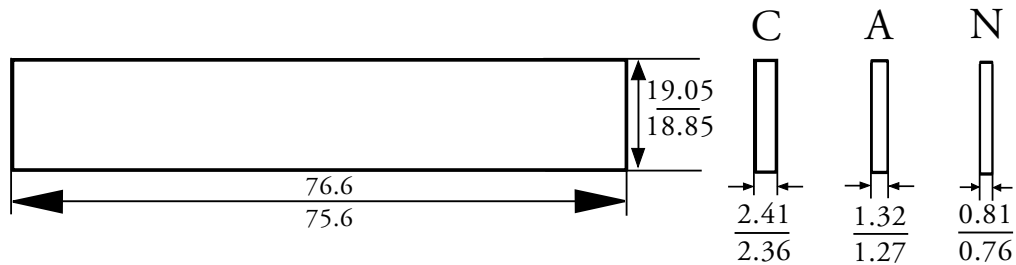
Figure 2.2 Maximal and minimal dimensions of the different Almen strips, in mm, as per SAE J442 [9]

Almen intensity has a significant influence on target's roughness, which increases with the intensity. Figure 2.3b shows the resulting residual stress field. The depth of the compressive layer is about 130 μm and the maximum of compressive stress is located 15 μm under the surface. The yield stress of Ti-6Al-4V is 880 MPa. It can be noted that the maximum compressive stress is about 93% of the yield stress.

It should be noted that no data was found for the shot peening of E-16NiCrMo13, or similar materials in the literature, in a range of Almen intensity close to that investigated in this work (0.12 mmA- 0.25 mmA).
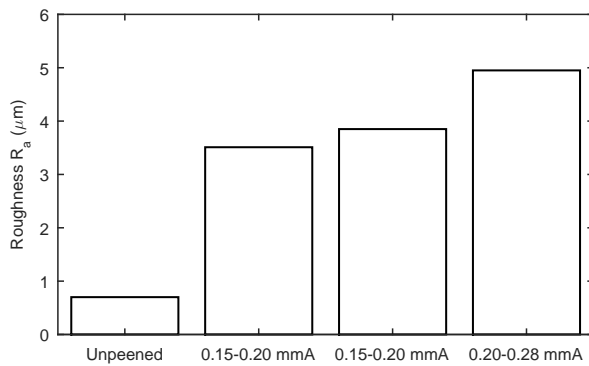
(a) Average roughness R_a of Ti-6Al-4V samples after shot peening at different intensities and 100% coverage [11]
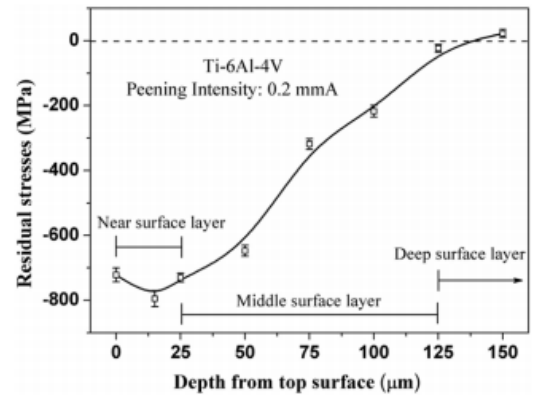
(b) Residual stress profile of Ti-6Al-4V samples after shot peening at 0.20 mmA and 100% coverage [12]

Figure 2.3 Resulting roughness and residual stresses after shot peening treatment

2.2 Vibratory finishing

2.2.1 Mass finishing processes

Mass finishing process simultaneously treats many components made of metal and other materials to induce effects like deburring, surface smoothing, edge break, stock removal, surface preparation, etc. Mass finishing processes have been used in the industry since the 1900s [13], but tumbling barrels have been found from the time of ancient Chinese and Egyptians. A mass finishing process consists in treating parts in a recipient filled with abrasive and/or non-abrasive media. A periodic motion is applied to the recipient, creating shocks and impacts between media and parts. These impacts alter the surface and sub-surface properties. The media can be lubricated to avoid heating the parts and to clean the dust from the polishing that could damage the surface.

Mass finishing is often required as a final treatment, either prior to final assembly for mechanical purposes or for aesthetic ones [1]. Mass finishing can also be part of the production line as a final step. Furthermore, these processes deliver highly consistent and repeatable results.

2.2.2 Vibratory finishing process

Vibratory Finishing (VF) has been used in the industry since the 1950s and widely accepted in the 1960s. However, very few scientific studies of the process can be found in the literature before 1975. A vibratory finisher consists in a container filled with media (Figure 2.4) and mounted on springs. A vibration generator is attached to the container and is constituted of one or two unbalanced shafts that are driven by a motor. Controlling the motor rotation speed, the mass of media, the stiffness of springs, etc, creates different vibration modes that fluidize the media. A mix of water and lubricant, which is called compound, is often added in the container and used to clean the media and parts. It also favors the flow circulation by lubricating the media bed and reduces the possible heat increase. Some compounds contain acids and are chemically reactive, which accelerates the metal finishing process [14]. The use of lubricant yields better surface finish because the media tends to slide more on the workpiece and the lubricant increases the contact surface, decreasing the abrasive effect. The nature of the media is an important key of the process and its choice depends on treatment's objectives [15]. There is therefore a wide range of shape, size, material and media roughness. Plastic, ceramic and steel media are the most widely used.

Two types of vibratory finishing processes are presented in Figure 2.4a (bowl-type) and

Figure 2.4b (tub-type). The bowl-type process creates a 3D media flow while the tub-type process creates a 2D flow. Tub-type processes can treat larger parts than the bowl-type process. Hashimoto et al. [16] studied the influence of eccentric weights disposition in a bowl-type finisher on media flow through analytical and experimental means. The authors proposed an optimal disposition (67° between the weights) to maximize machine performance and chose the average media velocity as the control parameter. Naeini et al. [17] studied the media flow in a tub-type finisher using transparent plates to create an easily observable one-ball layer. The authors used the same setup to study multiple layers of media [18]. They compared 2D discrete element simulations with experimental results and found that the model could predict the circulation trends quite accurately. They varied the number of shots in the system and could predict the shots velocities within 10% of experimenally measured values for 50 and 400 shots. Hashemnia et al. [19] studied the media flow of a tub-type finisher using a visco-plastic finite element continuum model. The authors implemented the model using parameters calculated from a discrete element model of the media bed. They demonstrated that a continuum model produced results comparable to a discrete model, with an average difference of 15% with experimental data, for one eight of the computational time.

(a) Bowl-type [20]   (b) Tub-type [21]
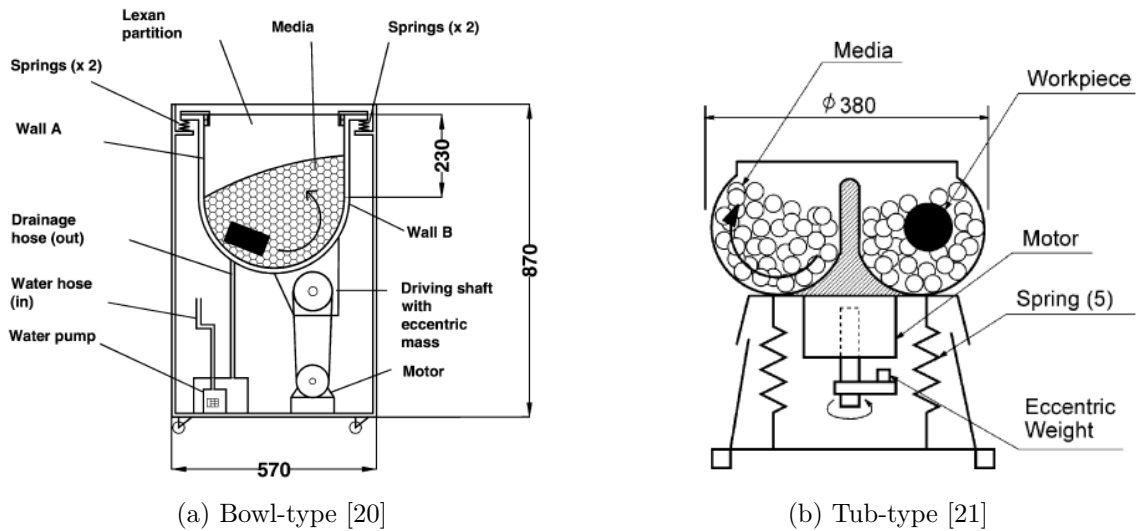
Figure 2.4 Different types of vibratory finisher, cross sections

2.3 Vibratory peening

2.3.1 Process presentation

The vibratory peening machine is a vibratory tub-type finisher where the part is fixed to the container, as shown in Figures 2.5 [22] and 2.6 [23] . The relative velocity between the media and the part is therefore increased, which leads to stronger impacts. The machine is composed of a container filled with spherical and non-abrasive media (to avoid stock removal), a suspension system (springs or airbags) and a vibration system (Figure 2.5). The vibration system induces a motion inside the machine, transmitting energy to the container and to the media. Vibrations are created using unbalanced shafts put into rotation by a motor and the amplitude of vibrations can be modified by changing the shafts' balance and the suspension stiffness. The vibrations frequency is controlled by the motor rotation speed and hardly goes above 60 Hz. Lubricant is sprayed through nozzles and cleans the media from dust and reduces heating. The impacts between the part and the media are mechanically plastifying its surface, which induces modifications in a subsurface layer.

Vibratory peening is relatively new and very few dedicated studies have been reported in the literature [3, 22, 23, 24, 25] so far. Some authors have developed numerical models for predicting the media dynamics [26, 27]. While these studies provide a sound scientific ground for a better understanding of the process, predicting its effects remains a challenge.
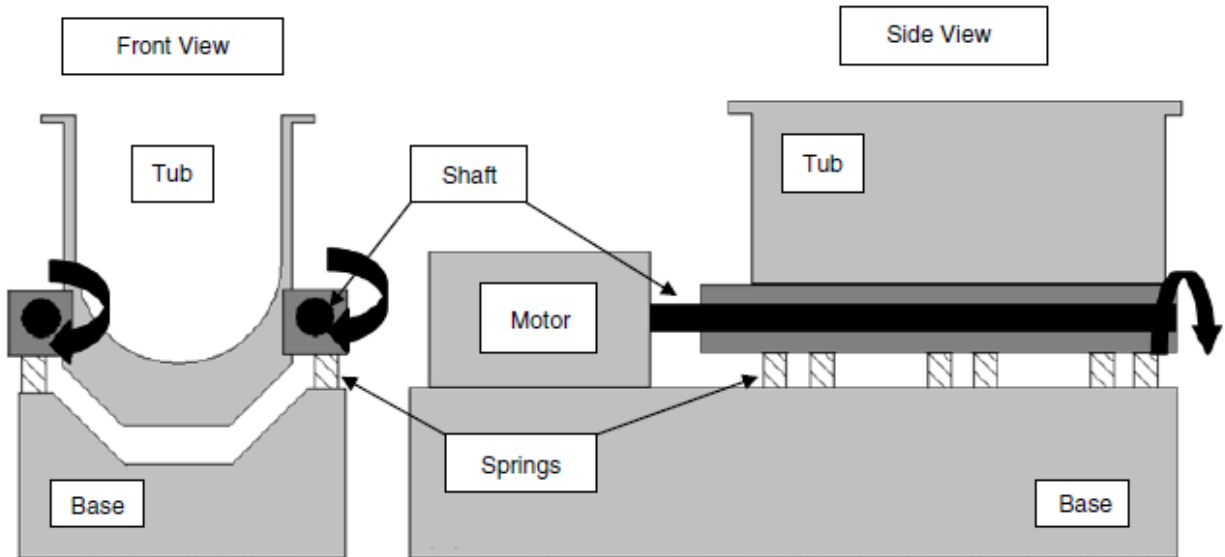
Figure 2.5 Schematic of a vibratory peening machine [22]

Figure 2.6 Picture of a strip holder inside the VP machine filled with steel media [23]

A number of authors also related the process parameters to resulting roughness, residual stresses and fatigue life [3, 22, 25]. These studies present the process' effects on aluminum alloys AA7050-T7451 and AA3003-H14 [22, 25], titanium alloy Ti-6Al-4V [24] and Inconel 718 [3]. Wang et al. vibratory peened a sintered 316LSC stainless steel and showed that the process increased the corrosion performance [28].

2.3.2 The use of Almen(-like) intensity and coverage in the VP process

Baghbanan et al. [20] vibratory peened aluminum (AA6061 and AA1100) and copper strips similar to Almen strips. The authors showed lubricant trapped between the strip and the holder increases the strip's stiffness, leading to a greater curvature than applying the process in dry conditions. This observation suggests that care must be taken if lubricant is found beneath the strip after processing.

Ciampini et al. [23] relied on Almen-like aluminum strips to characterize the VP process. The strips were vibratory peened under different processing conditions and impact velocities have been measured with a force sensor. The authors observed that higher impact velocities led to higher arc heights and concluded that the adapted Almen system was appropriate to characterize the process' efficiency.

Ciampini et al. [29] developed a model for predicting the curvature of vibratory peened

aluminum strips. The authors used the finite element technique to calculate curvature as a function of residual stresses distribution. They found that curvature was a unique function of cumulative absorbed energy for a given set of ball radius, material model and strip thickness.

The fact that authors relied on Almen-like strips not made of standardized SAE 1070 steel makes the comparison of resulting residual stresses and roughness with those of conventional shot peening impossible. Therefore, the question of the capability of the VP process to reach intensities comparable to those used in aerospace industries has yet to be addressed.

2.3.3 Comparison of VP and VF in terms of surface characteristics and fatigue lives.

Gane et al. [24] compared the fatigue lives and roughness of Ti-6Al-4V flat notched samples ($K_t = 1.5$) treated with VF and VP. VP was realized with a mixture of 4 to 7 mm diameter hardnened steel balls. The vibrations amplitude was of 4 mm and the processing time was one hour. The VF process used 10 mm triangular ceramic abrasive media. The amplitude of vibrations was 2.5 mm and the processing time was one hour. Fatigue tests were carried out at a maximum stress of 458 MPa (52% of the yield stress), a stress ratio R=-0.2 and a frequency of 20 Hz. The authors observed that VP led to a 104% High Cycle Fatigue (HCF) life improvement, when compared to that obtained with VF. Furthermore, VP reduced the scatter in the fatigue testing results, when compared to VF. The authors measured residual stresses and found that the maximum compressive stress was 41% higher for VP, when compared to VF. This is explained by a higher energy transmitted to the parts due to higher impacting velocities. Furthermore, the maximum compressive stress was deeper and the position where the profile became positive was deeper as well for VP, when compared to that resulting from VF. The roughness measurement showed that average roughness parameter R_a was 8% higher with a lower scatter in VP than that observed in VF.

This study suggests that VP can potentially lead to better HCF lives than VF. This result could be explained by the fact that the surface finish was almost identical for both processes while VP induced more compressive residual stresses than VF.

2.3.4 Comparison of VP and SP in terms of surface characteristics, residual stresses and fatigue lives.

Gane et al. [24] compared the effects of different surface treatments in terms of fatigue life, roughness and residual stresses on Ti-6Al-4V plates. The authors treated and fatigue tested flat notched specimens ($K_t = 1.5$). The samples underwent fatigue tests at a maximum stress

of 458 MPa (52% of the yield strength), a stress ratio R=-0.2 and a frequency of 20 Hz. They compared vibratory deburring (VD), shot peening at two different intensities (0.18 mmA and 0.43 mmA) and vibratory peening. VD is similar to VP since the part is fixed in the tub and the only difference is that the authors used ceramic media for VD and steel media for VP. VP and VD led to similar roughness R_a, about 75% lower than SP at 0.18 mmA and 90% lower than SP at 0.43 mmA. The residual stresses resulting from the application of VP were very close to those resulting from shot peening, but went deeper (+40% at -50 MPa), when compared to SP at 0.18 mmA. SP at 0.43 mmA induced higher residual stresses, when compared to VP. The VP samples had HCF lives similar to those of samples shot peened at an intensity of 0.43 mmA, for a lower scatter. However, the VP samples had better HCF lives than those shot peened at an intensity of 0.18 mmA. The VD samples had a large scatter and an average HCF lower than that of SP samples.

Sangid et al. [22] compared the effects of SP and VP on AA7050-T7451 samples in terms of roughness, residual stresses and fatigue life. The authors treated and studied flat notched specimens having a stress concentration factor $K_t = 1.5$. The samples were tested in HCF at a maximum stress of 284 MPa (61% of the yield stress), a stress ratio R=0.1 and a frequency of 2 Hz. VP led to a better fatigue life with a larger scatter, when compared to that obtained from SP. The integral of the compressive residual stresses was higher for SP than for VP (+80%) while the roughness parameter R_a was higher for SP(+250%). SP led to higher roughness because its highly energetic impacts occurred on small area and induced deep dimples. By opposition, the VP process relies on larger shots traveling at lower velocities, which leads to wider and less deep craters.

Feldmann et al.[3] compared the VP and SP processes effects on full blisk-rotors made of a nickel based alloy. The authors studied two kinds of media: a "hard media" and a "soft media" (the media material was not disclosed in their works). It was found that the VP process led to an average roughness R_a of 0.15 μm when using the hard media and 0.21 μm when the soft media, while shot peening led to an average roughness of 0.41 μm. Residual stresses measurements showed that applying the VP process with hard media yielded compressive stresses in the subsurface layer similar to those obtained from SP. Surface compressive residual stresses were higher after SP (+13%). However, the higher compressive stresses were similar for both processes and the residual stress profile resulting from VP was deeper (+85% at 5% of the maximum stress), when compared to SP. The samples treated with soft media showed a lower high cycle fatigue strength than samples treated by SP (-16%). Note that the fatigue results obtained with the hard media were not presented.

This somewhat limited survey suggests that shot peening led to globally higher compressive stresses but vibratory peening yielded much better surface finishes. Shot peening yielded

better or similar fatigue lives than vibratory peening. However, most of these studies did not compare processes of similar intensities, which implies that these observations must be confirmed by more rigorous studies.

2.4 Influence of VP process parameters on the process's effects

2.4.1 Roughness

Roughness parameters like the average roughness R_a, the skewness R_{sk}, the kurtosis R_{ku}, the mean peak width RS_m and the total height of the profile R_t, are calculated as

$$
\begin{aligned}
R_a &= \frac{1}{l_s} \int_0^{l_s} |Z(x)| dx; \\
R_q &= \frac{1}{l_s} \int_0^{l_s} Z^2(x) dx; \\
R_{sk} &= \frac{1}{R_q{}^3} \frac{1}{l_s} \int_0^{l_s} Z^3(x) dx; \\
R_{ku} &= \frac{1}{R_q{}^4} \frac{1}{l_s} \int_0^{l_s} Z^4(x) dx; \\
RS_m &= \frac{1}{m} \sum_{i=1}^{m} X_{Si}; \\
R_t &= \max_{l_a} Z - \min_{l_a} Z
\end{aligned}
\tag{2.1}
$$

where Z is the profile's height, l_s the sampling length, l_a the acquisition length ($l_a = 5l_s$). $\{X_{Si}, i \in [1, m]\}$ is the ensemble of profile elements within l_s. Some of these parameters are schematized in Figure 2.7.

Hashimoto [30] developed an analytical model to predict average roughness R_a evolution as a function of time as
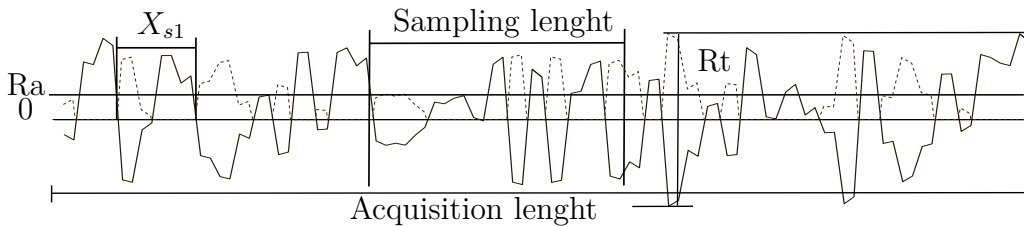
Figure 2.7 Schematization of R_a, RS_m and R_t parameters on a profile

$$R_a(t) = (I_r - D_r)e^{-\frac{t}{T}} + D_r \tag{2.2}$$

where D_r is the roughness threshold, I_r is the initial roughness and T is a time constant that depends on process parameters. This model is based on the fact that a threshold roughness D_r exists and is intrinsic to the VP process, and that the roughness evolution rate increases when the difference between actual R_a and D_r increases. The threshold roughness not only depends on the working material and media properties, but also on machine properties. According to this model, increasing the processing time should not degrade the surface roughness.

Domblesky et al. [31] vibratory finished aluminum, brass and steel parts using ceramic rough media and obtained results in agreement with Hashimoto's model. Walton et al. [32] vibratory peened Ti-6Al-4V samples in a bowl type finisher for different processing times. The authors showed that the surface roughness evolution was well represented with Hashimoto's model.

Sangid et al. [22] studied the influence of vibrations frequency and amplitude on roughness. The authors treated 7050-T7451 aluminum samples in a tub-type machine with ceramic media. Their analysis showed that increasing vibrations frequency increased roughness (R_a of 0.75 μm at 20 Hz and of 0.83 μm at 32 Hz). It also showed that increasing vibrations amplitude yielded a slightly rougher surface (R_a of 0.77 μm at 2.4 mm and of 0.81 μm at 2.8 mm).

Wang et al. [33] investigated the lubrication and the media roughness effects on the roughness of vibratory finished part. The authors treated aluminum AA1100-O and AA6061-T6 samples in a bowl-type machine with ceramic media. The authors found that vibratory finishing under dry conditions led to higher roughness (R_a of 2.35 μm, using 9 mm ceramic media and after processing AA 1100-O samples for 80 minutes) than vibratory finishing under lubricated conditions (R_a of 0.56 μm, using 9 mm ceramic media and after processing AA1100-O samples for 80 minutes). The authors investigated the effect of media roughness on parts roughness using ceramic media having different surface characteristics (R_a=15.4 μm; R_{sk}=-0.43 and R_a=13.8 μm; R_{sk}=-0.156). The authors concluded that the rougher media led to a higher roughness (R_a=2.36 μm after processing AA1100-O samples for 80 minutes under dry conditions), when compared to the smoother media (R_a=0.58 μm after processing AA1100-O samples for 80 minutes under dry conditions).

Feldmann et al. [3] treated full blisk-rotors made of a nickel based alloy with the VP

process and found that hard media led to lower roughness (0.15 μm), when compared to that resulting from the use of soft media (0.21 μm).

2.4.2 Hardness

Wang et al. [33] studied hardness evolution of vibratory finished AA1100-O and AA6061-T6 samples. The authors treated AA1100-O and AA6061-T6 samples under dry and detergent-wet conditions and found that the dry condition led to higher hardness with a greater scatter (146 HV on AA6061-T6 vibratory finished for 80 minutes), when compared to lubricated conditions (116 HV on AA6061-T6 vibratory finished for 80 minutes). The authors investigated the effect of media roughness on hardness using ceramic media having different surface characteristics (R_a=15.4 μm; R_{sk}=-0.43 and R_a=13.8 μm; R_{sk}=-0.156). The studies suggest that the rougher media led to a higher hardness increase (+13 HV on AA1100-O vibratory finished samples for 80 minutes under wet conditions), when compared to the smoother media (+4 HV on AA1100-O vibratory finished samples for 80 minutes under wet conditions). Globally, hardness increased with the processing time, but few experiments showed a hardness decrease after a certain processing time. The same materials were investigated by Baghbanan et al. [20]. The authors concluded that hardness globally increased with processing time but observed some exceptions as well.

2.4.3 Residual stresses

Few authors investigated the residual stresses resulting from vibratory finishing / peening processes. Feldmann et al. [3] measured the residual stress field after processing airfoils made of a nickel based alloy with a bowl type vibratory peener. They used soft and hard media and showed that hard media induced deeper and more compressive residual stresses. Sangid et al. [22] measured residual stresses profiles in vibratory peened samples made of 7050-T7451 aluminum under different conditions. The authors used the integral of the profile to present their results. That scalar can also be a measure of the total strain energy. The authors found that frequency had a strong influence on that parameter. An increase of processing frequency led to an increase of compressive residual stresses. The influence of amplitude was found to be insignificant on the residual stresses integral. The authors also observed that samples having the most compressive residual stresses were also those with the worst surface finish. The authors have also shown that normal impacts, when compared to tangential impacts, produced larger residual stresses, but rougher surfaces. Ciampini et al. [34] treated AA6061-T6 disks equipped with sensors under different mass of media and material conditions and measured the impacting forces. The authors found that reducing the mass of media from

112 kg to 91 kg led to a more energetic process. The author related this phenomenon to the increase of vibrations amplitude.

2.4.4   Fatigue life

Sangid et al. [22] shot peened and vibratory peened flat notched specimens having a concentration factor $K_t = 1.5$. The samples were made of AA7050-T7451. They were tested in HCF at a maximum stress of 284 MPa, a stress ratio R=0.1 and a frequency of 2 Hz. The authors found that all the vibratory peened samples had a higher fatigue life than the shot peened samples. The authors found that the VP processing conditions had a strong influence on the fatigue life results. For example, using rough ceramic media was shown to increase the scatter in the fatigue life results, when compared to worn ceramic media. The authors have also varied the samples positions and orientations and found that normal impacts induced the best fatigue life improvement, despite the fact they produced the roughest surfaces.

2.4.5   Summary

Table 2.1 summarizes the influence of machine parameters on roughness, residual stresses and hardness.

Table 2.1 Effects of processing parameters on residual stresses, roughness and hardness

Machine parameters	Residual stress	Roughness	Hardness
Processing time	+	-	+
Amplitude	+	?	n/a
Frequency	+	?	n/a
Lubrication	n/a	-	-
Media hardness	+	?	+
Media roughness	n/a	?	+
Media size	n/a	n/a	?
Legend	+ = an increases induce an increase - = an increase induces a decrease ? = no trend can be observed from data n/a = no data available		

CHAPTER 3   ANALYSIS OF LITERATURE AND OBJECTIVES

The literature survey led to the following findings:

- The effects of VP have been studied on very few alloys, namely aluminum AA7050-T7451 and AA3003-H14, titanium Ti-6Al-4V, a nickel based alloy and sintered 316LSC stainless steel.

- Processing time, amplitude, frequency, lubrication, media hardness, roughness and size, part's position and orientation within the tub have been shown to have an influence on residual stresses, roughness and hardness. However, the limited amount of publicly available studies prevent from drawing general and rigorous conclusions.

- Vibratory peening induces compressive residual stresses beneficial for fatigue life (crack closure mechanism) and yields much better surface finish than shot peening.

- Almen(-like) intensity has been demonstrated as a relevant control parameter for VP. However, the use of standardized Almen strips has not been reported in the literature. Therefore, the range of Almen intensities attainable by the process has yet to be determined.

- The effects of VP and SP processes have not been compared using a common control parameter (as Almen intensity, for example).

- Very few studies have demonstrated the fatigue life improvement resulting from vibratory peening.

These observations rise the following questions:

1. Is the vibratory peening process able to achieve a range of Almen intensities comparable to those obtained from the shot peening process ?

2. What are the effects of vibratory peening on roughness, residual stresses and hardness for aerospace materials ?

3. Could vibratory peening be an efficient process for fatigue life improvement ?

The following specific objectives were defined to address these questions:

1. Demonstrate the capability of the vibratory peening process to reach Almen intensities in the range of 0.12 mmA and 0.25 mmA, which is the range typically used in aerospace.

2. Study the influence of vibratory peening on roughness, hardness and residual stresses for Ti-6Al-4V and E-16NiCrMo13. These materials were chosen by Safran and are used in landing gears and airplane engines.

3. Compare the effect of vibratory peening and shot peening processes for similar Almen intensities.

All these objectives are addressed in Chapter 4. Chapter 4 is a journal paper submitted to the Journal of Materials Processing Technology on the 2018/01/27. The authors are Jawad Badreddine, Brian McGillivray, Hong Yan Miao, Martin Lévesque and myself as first author. My role in this paper was to carry out all the experiments and lead the paper's writing. The other authors supervised the works. My contribution to this paper has been evaluated to 90%.

CHAPTER 4 ARTICLE 1: EFFECT OF VIBRATORY PEENING ON THE SUB-SURFACE LAYER OF AEROSPACE MATERIALS Ti-6Al-4V AND E-16NiCrMo13

Léo Canals, Jawad Badreddine, Brian McGillivray, Hong Yan Miao and Martin Lévesque. Submitted to *Journal of Materials Processing Technology* on January 27, 2018.

4.1 Abstract

Conventional Shot peening (SP) is a widely used fatigue life improvement process by impacting the metal component with high velocity shots. The plastic deformation induces a layer of compressive residual and cold work which retards the crack initiation and propagation. However, shot peeing increases surface roughness which acts as stress concentrator and decreases fatigue life. Vibratory finishing (VF) is a mass finishing process in which components are inserted in an oscillating bowl, or tub, containing polishing media. The media flow around the component polishes its surface and decreases its roughness. Vibratory peening (VP) is a modified vibratory finishing process that induces compressive residual stresses comparable to those induced by shot peening, but for a much better surface finish. In this paper, the effects of vibratory peening on surface roughness, residual stresses and hardness were investigated on two aerospace materials, titanium alloy Ti-6Al-4V and carburized steel E-16NiCrMo13. Studied process parameters are frequency, media mass and processing time. A study of Almen intensity as a function of machine parameters has been carried out to define the machines' parameters leading to the target Almen intensities of 0.12 mmA, 0.18 mmA and 0.25 mmA. The influences of media mass and frequency on peening intensity have been investigated. The study results show that the VP process can deliver the targeted intensities consistently. Roughness measurements show that for both studied materials, VP produces good surface roughness with a consistent average roughness value in the range of 0.3-0.4 μm. The residual stress profiles produced by VP are comparable to which produced by conventional SP at same Almen intensity. Compared to conventional SP, VP led to higher maximum compressive values for steel and equal for titanium, while deeper depths of the compressive region (+126% for steel). Hardness measurements show that VP has limit influence on a layer with depth of 70 μm. In general, the VP process is capable of consistently produce a beneficial layer of compressive residual stress together with a good surface finishing which could greatly improve fatigue properties on aerospace components.

4.2   Keyword

Vibratory peening, residual stresses, roughness, hardness, fatigue life

4.3   Introduction

Conventional shot peening consists in projecting hard particles at high velocity onto a ductile metallic surface. The process induces compressive residual stresses, hardening and microstructural changes that delay fatigue crack initiation and propagation. The process also increases surface roughness, which increases stress concentration and is detrimental for fatigue life. Shot peened parts are often subjected to surface finishing treatments like vibratory finishing, low intensity peening [35] or peening with smaller shots [36] to improve their surface characteristics.

The conventional shot peening process is specified mainly by two process variables: Almen intensity and coverage. The Almen intensity is related to the kinetic energy, per second, transferred to the part and is measured by submitting a thin standardized steel strip (SAE J442 [9]), held in a standardized Almen holder, to the process. The residual stresses induced by the process progressively bend the strip and its arc height is measured with a standardized Almen gage as a function of the peening time. The Almen intensity is defined as the arc height when doubling the peening time increases the arc height by 10%. Almen strips come in three types of various thicknesses, namely A (1.3 mm), C (2.38 mm) and N (0.79 mm). Coverage is related to the peening time and is defined as the ratio of the surface covered by dimples over the total treated surface. 98% coverage is referred to as full coverage and any coverage value above 100% is a multiple of the peening time required to reach full coverage.

Vibratory Finishing (VF) is a mass finishing process in which components are inserted in an oscillating bowl, or tub, containing polishing media. The vibrations create a flow in the media that abrades and polishes the parts. The process has been developed in the 1950s and widely applied since the 1960s [37]. In addition to improve surface finish, the process induces compressive residual stresses of lower intensity than those resulting from shot peening [24]. The process effects in terms of material removal [31], roughness [20], edge rounding [38] and hardness [33] have been studied in the open literature.

Vibratory Peening (VP) is a process derived from vibratory finishing that consists in inserting a fixed part into an oscillating bowl filled with polishing media. The relative movement between the treated parts and media is significantly increased and leads to higher impact velocities, when compared to VF. The process induces surface modifications in a small sublayer of about 400 micrometers [22]. The process is somewhat similar to conventional shot

peening in the sense that the impacting media induces compressive residual stresses [25] and work hardening [33]. However, the VP process results in a much smoother surface finish than SP. The process could therefore be a potential candidate to either combine peening and polishing into a single step or even to improve fatigue life, when compared to conventional shot peening.

The VP process is relatively new and few dedicated studies have been reported in the literature since the 2000s, mostly through conferences proceedings. Some authors adapted the Almen intensity system used with the SP process to the VF and VP processes. Ciampini et al. [23] used aluminum 3003-H14 strips, similar in length and width to Almen strips (as per SAE J442 [9]) but with two different thicknesses. One thickness corresponded to the N strip and the other one was thinner (0.62 mm). The authors used these strips to characterize the VP process' relative aggressiveness with the change of the sample's position within the tub and the mass of media. Baghbanan et al. [20] also used aluminum strips (AA6061 and AA1100) and copper strips to characterize the VF process intensity. By varying the lubrication conditions, the authors found the use of lubricant led to higher peening intensities. They found that applying a grease film between the strips and the holder led to higher curvatures under dry conditions, when compared to strips without the grease film. The authors confirmed that wet conditions were less aggressive (the impact strength is reduced by the presence of a lubricant film between the part and the media), but gave higher peening intensities due to lubricant behind the strips, when compared to dry conditions.

Gane et al. [24] compared the fatigue lives and roughness of Ti-6Al-4V samples peened with SP and VP. The authors treated and fatigue tested flat notched specimens ($K_t = 1.5$). Samples were shot peened at 0.18 mmA and 0.43 mmA, with 100% coverage, using CS 280 hard cast steel shots. VP was performed with 4 to 7 mm diameter hardened steel ball bearings for one hour. The samples underwent fatigue tests at a maximum stress of 458 MPa (52% of the yield strength), a stress ratio (minimum stress over maximum stress) R=-0.2 and a frequency of 20 Hz. The authors observed that VP led to a 12% High Cycle Fatigue (HCF) life improvement (2.1×10^5 cycles), when compared to the fatigue lives obtained after shot peening at an intensity of 0.43 mmA (1.9×10^5 cycles). Furthermore, VP reduced the scatter in resulting fatigue lives, when compared to SP. The authors also measured residual stresses and found that the maximum compressive stresses were of the same magnitude of those resulting from SP at an intensity of 0.18 mmA. However, the residual stresses induced by VP were deeper in the affected layer than those induced by SP.

Sangid et al. [22] experimentally studied the impact of VP on the roughness, the residual stresses and the fatigue life of AA7050-T7451 samples. The authors treated and studied flat

notched specimen having a stress concentration factor $K_t = 1.5$. The samples were tested in HCF at a maximum stress of 284 MPa (61% of the yield stress), a stress ratio R=0.1 and a frequency of 2 Hz. The authors found that low tub frequency and vibrations amplitude yielded better surface finish, while high tub frequency and vibrations amplitude led to more important residual stresses, which in this specific case, led to higher fatigue lives in HCF conditions. The authors also found that the part's position and orientation within the tub had a significant influence on fatigue life, roughness and residual stresses measurements. Moreover, the authors compared the fatigue life enhancement resulting from the VP process to that resulting from the SP process. The authors averaged the fatigue lives of samples vibratory peened (without providing Almen intenity measurements) to samples shot peened at an intensity of 13 mmA (the media used for the SP process was not specified). The authors found that VP led to a 62% fatigue life improvement(1.5 x 10^5 cycles), when compared to SP performed at an intensity of 13 mmA (9 x 10^4 cycles).

This literature survey reveals that processing time, amplitude, frequency, mass and type of media, lubrication intensity, position of the part and its orientation in the tub influence the process effects in terms of residual stresses, roughness and fatigue life. In addition the range of Almen intensities that could be reached by the process has not been studied yet, to the best of our knowledge. This information is very important from an industrial stand-point because it would provide common bases to compare VP effects to those of the widely accepted and standardized SP process. Moreover, to the best of our knowledge, VP-induced hardness variations have never been studied. Hardness is a key driver in fatigue life and having this information would provide sound grounds to assess the process' potential to improve fatigue. Finally, the number of studies related to the application of VP on titanium is somewhat limited and non-existent on steel alloys.

Sangid et al. [25] used the measurements of media velocities and frequencies from [22] to simulate the evolution of coverage with time. The authors used aluminium alloy AA7075-T6 properties for their model. They found that for a frequency of 32 Hz, the processing time to reach 95% coverage was of 40 minutes while it was of 60 minutes to reach 99%. The authors concluded that the effects of the VP process saturated after 60 minutes.

The principal objectives of this work were to investigate the range of Almen intensities that can be reached by the process and study its effects, in terms of roughness, residual stresses and hardness on TI-6Al-4V titanium and E-16NiCrMo13 cemented steel alloys. These two alloys are mainly used in gas turbine engines and landing gears and were identified as potential candidates to benefit from the VP process. Section 4.4 presents the materials and methods used in this study. Section 4.5 presents the study of Almen intensity as a function of

process parameters. Section 4.6 presents the effects of the VP process on roughness, residual stresses and hardness, for the two selected materials. The results are then discussed in Section 4.7 and Section 4.8 concludes the work.

4.4 Materials and methods

4.4.1 Materials

The Almen strips processed in this study were A-type strips($76 \times 19 \times 0.8$ mm^3), 1-S-grade (hardness 450 -490 HV), as specified in standard SAE J442 [9].

A case hardened low alloy steel E-16NiCrMo13 and a titanium alloy Ti-6Al-4V (ASTM 4911N standard) were used for this study. Their chemical compositions are specified in Table 4.1. The Ti-6Al-4V alloy was provided as 8 mm thick laminated plates at an annealed condition, according to the AMS4911N standard [1]. The obtained microstructure is an alpha-beta alloy (Figure 4.1) with a surface and bulk hardness of 350 $HV_{0.1}$. Its mechanical properties are given in Table 4.2. The E-16NiCrMo13 steel was provided as normalized and annealed 190 mm bars, from which all specimens were extracted and machined. The specimens were then case hardened with low-pressure carburizing equipement, and gas quenched. A cryogenic treatment was applied to reduce residual austenite. Finally, a stress relieve treatment was done to achieve a surface hardness of 750 $HV_{0.3}$ and a bulk hardness of 400 $HV_{0.3}$ at a depth of 1.5 mm from the surface. This represents a carbon concentration gradient, with around 0.7%w at the surface (before grinding) and 0.17%w at the bulk. The obtained microstructure, presented in Figure 4.2, shows martensitic microstructures gradually etched (due to the carbon gradient) representative of that usually observed in case hardened steels. The mechanical properties of the bulk material are also given in Table 4.2.

Fifteen Ti-6Al-4V samples having dimensions of $60.0 \times 18.9 \times 8.0$ mm^3 and fifteen E-16NiCrMo13 samples having dimensions of $79.9 \times 18.9 \times 8.0$ mm^3 were submitted to the VP process. The steel specimens were grinded after the case hardening, resulting in an average roughness R_a of 0.7 μm. The titanium specimens were milled ($R_a \approx 0.4$ μm). The samples were made thicker than Almen strips to reduce the bending induced by the process.

Table 4.1 Chemical composition of the Ti-6Al-4V titanium Alloy (AMS 4911) and the carburized E-16NiCrMo13 low alloy steel (ISO 683-17 Grade 16NiCrMo13)

Wt. %	Fe	Ti	Al	V	Ni	Cr	Mo	C	Mn	Si	P	S	Cu	O
Ti-6Al-4V	<0.25	Balance	6	4	-	-	-	-	-	-	-	-	-	<0.2
E-16NiCrMo13	Balance	-	-	-	3.5	1.1	0.3	0.17	0.6	0.4	0.025	0.02	0.35	-
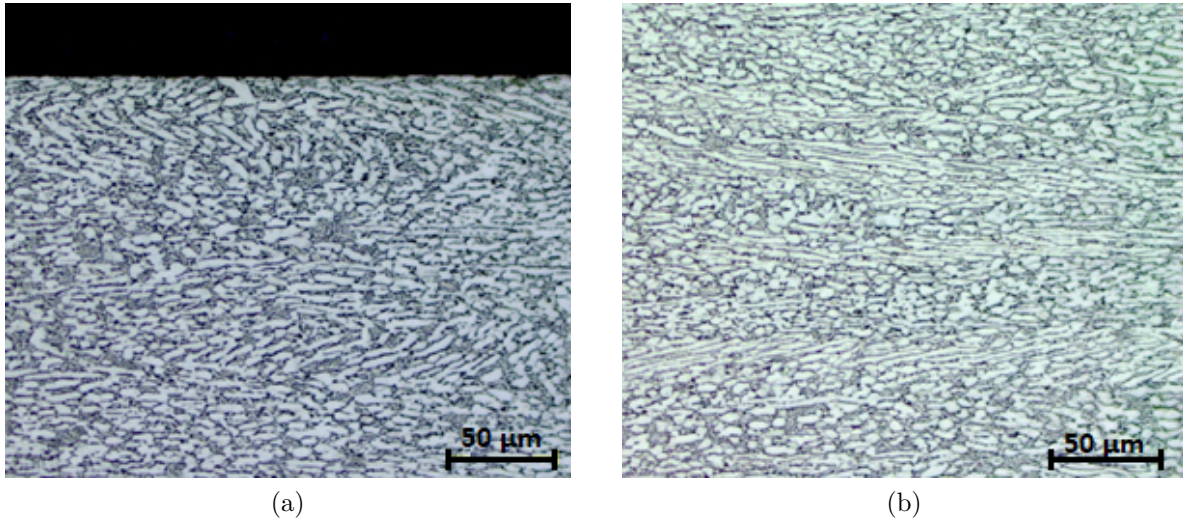
Figure 4.1 As received microstructure of annealed Ti-6Al-4V titanium alloy at surface (a) and at bulk (b)
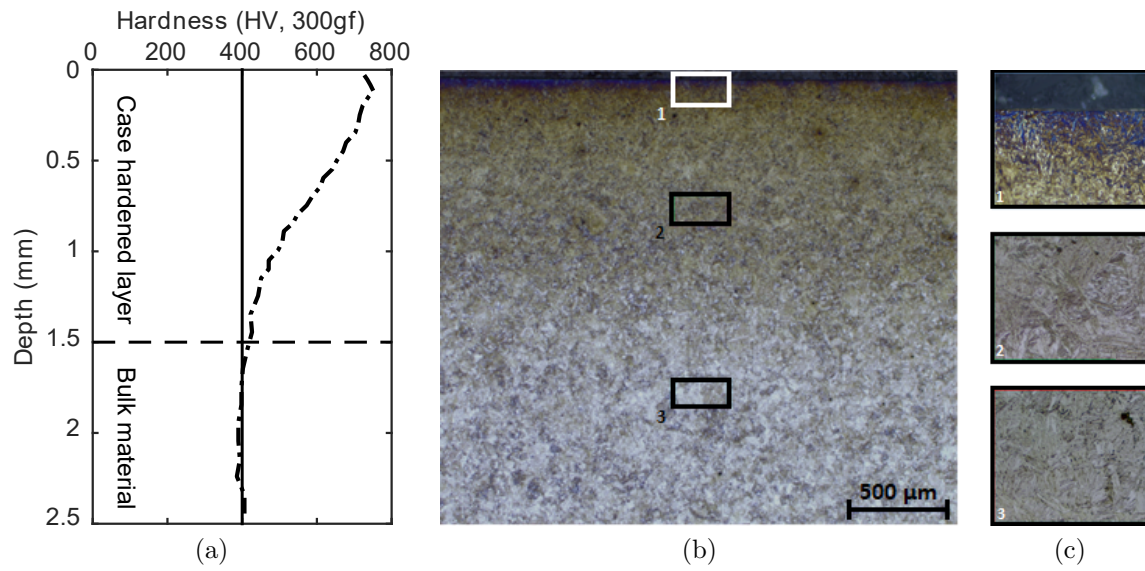
Figure 4.2 (a) Micro-hardness (b,c) and microstructure gradients of case hardened E-16NiCrMo13 steel

Table 4.2 Ti-6Al-4V titanium alloy [39] and carburized E-16NiCrMo13 low alloy steel properties (ISO 683-17 Grade 16NiCrMo13)

Properties	Ti-6Al-4V	E-16NiCrMo13
Young Modulus (GPa)	114	210
Poisson ratio	0.23	0.28
Density (kg/m^3)	4430	7850
Yield Stress at 0.2% (MPa)	880	1000
Ultimate stress (MPa)	950	1350
Surface/Bulk hardness (HV)	350/350	750/400

4.4.2 Vibratory peener and media

A tub type machine built by Vibra Finish Ltd., as schematically depicted in Figure 4.3, was used to treat the samples. Figures 4.4, 4.5 and 4.6 show the actual machine used in the experiments. The oscillatory motion resulted from rotating shafts mounted with eccentric masses. The shafts rotated at the same frequency but in opposite direction. This configuration induced a vertical motion, as shown in Figure 4.3. The tub was mounted on airbags whose pressure was adjusted to control the vibration amplitudes and to ensure the tub's level. The tub was filled with media and the samples were firmly held in place in a four-strip holder setup shown in Figures 4.4 and 4.5. The pressure in the right-hand side airbags was set 69 kPa (10 psi) higher than that in the left-hand side airbags (Figure 4.6) to ensure the tub's horizontality (the tub is not balanced due to vibration system). The airbags pressure could be adjusted in the range of 103 kPa (15 psi) to 414 kPa (60 psi). The applied frequency ranged between 1 Hz and 60 Hz.

The tub was filled with AISI Type 1018 carbon steel balls having diameters of 3.18 mm (1/8 in), 4.76 mm (3/16 in) and 6.35 mm (1/4 in) in equal mass proportions (i.e., each ball size accounted for 1/3 of the total media mass). The carbon steel balls had a minimum hardness of 60 HR_c. The total media mass varied between 555 kg (1222 lbs) and 792 kg (1745 lbs). The machining coolant Castrol Syntilo^{TM}9828 (a water-based rust inhibitor) mixed with water (50% lubricant to water ratio) was sprayed with 2 nozzles on the media with a flow rate of 1.9 L/min. This compound also served as a media lubricant.

4.4.3 Shot peening

Two specimens for each materials were shot peened intensities of at 0.12 mmA and 0.18 mmA, respectively, with a surface coverage of 125%. The shot peening was conducted using ASR130 steel media (48-52 HR_c), projected through a 10 mm straight cylindrical nozzle, at
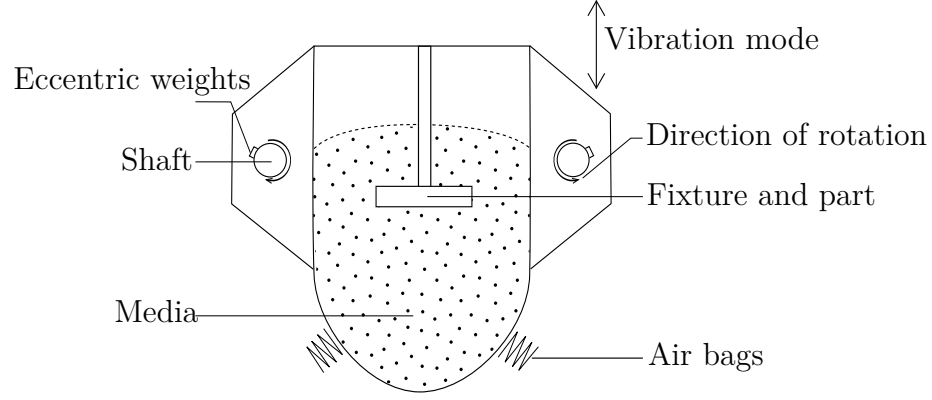
Figure 4.3 Schematic representation of the vibratory peening machine, front view. The unbalanced shafts rotate and induce the tub's vibrations. The movement sets the media into an up and down motion. The media impact the part, inducing the peening and finishing effects

an angle of 85° and a working distance of 180 mm from the specimens surface.

4.4.4   Instrumentations and methods

The mass of media used in the experiments was measured with a scale accurate to 0.227 kg (0.5 lbs). The machine's vibratory frequency was controlled on its interface by changing the rotatory frequency and the related sensor was accurate to 0.1 Hz. Lubrication was controlled through a flow regulator that adjusted the mixture of water and compound. A four-strips holder was used to simultaneously process multiple strips and samples. A preliminary study revealed that every specimen in the strip holder is subjected to the same peening treatment. Four Almen strips were peened simultaneously for the study presented in section 4.5 while positions A and D (Figure 4.5) were filled with Almen strips to protect the blocks, position B was filled with a E-16NiCrMo13 sample and position C with a Ti-6Al-4V sample in the study presented in Section 4.6.

Almen intensity was measured as per SAE J443 [8] standard on A strips with an Almen gage. The saturation curve was fitted from four arc height measurements, as per standard SAE J2597 [41] as,

$$h = a(1 - \exp^{-bt}) \tag{4.1}$$

where h was the arc height, t the peening time while a and b were least squares fitting parameters.

Coverage could not be measured as the surface finish was too smooth to identify dimples.

Regarding vibratory peened samples, roughness measurements were performed with a

Figure 4.4 4-strips holder, flush with media surface
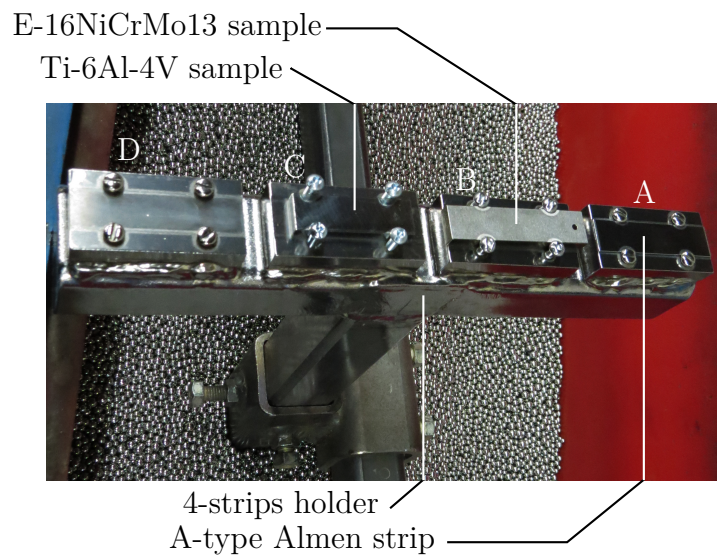
Figure 4.5 4-strips holder, with different types of specimens. Letters correspond to positions on the strips-holder

Figure 4.6 Actual vibratory peening machine, running with cover

Mitutoyo SV-C4000 series profilometer (resolution of 0.05 μm). Regarding shot peened samples, roughness measurements were performed with an Alicona InfiniteFocus G5 microscope by focal variation. Five surface roughness profiles were measured at different locations along the samples major length, for each vibratory peened sample (ten profiles for shot peened ones). In accordance with DIN EN ISO 4288: 1998 standard, a cut-off length of 0.8 mm and a total measured length of 4 mm were selected for vibratory peened samples (cut-off length of 0.8 mm and total length of 8 mm for shotpeened ones) as the roughness was expected to lie between 0.1 μm and 2 μm. Roughness parameters were calculated as per ISO 4287. The calculated parameters were R_a, the average profile roughness (mean of the absolute value of the profile height), R_{sk}, the profile skewness which measures its asymmetry, R_{ku}, a measure of the profile sharpness and related to the flattening of the surface, RS_m, a spacing parameter which measures the mean profile width distribution and R_t, the total profile height. A skewness value $R_{sk} < 0$ means that there are more valleys than peaks while $R_{sk} > 0$ means the opposite. A value of $R_{ku} > 3$ corresponds to a spiked surface while $R_{ku} < 3$ corresponds to a bumpier surface with rounded peaks.

Samples surfaces were observed under an optical microscope with 6.7X lens.

Residual stresses measurements of vibratory peened samples were carried out by American Stress Technologies Inc. with a goniometer Stresstech Xstress 3000 G2R, 7257/7258. The measurements were made according to ISO EN15305, ASTM E915-16 and SAE HS-784 standards. The diffractometer was equipped with a Ti-tube ($\lambda = 0.275nm$) and with a Cr-tube ($\lambda = 0.299nm$), respectively, for Ti-6Al-4V and E-16NiCrMo13 samples. For the shot peened samples, the measurements were carried out with a goniometer Brüker D8 Omega. The diffractometer was equipped with a Cu-tube and with a Cr-tube, respectively, for Ti-6Al-4V and E-16NiCrMo13 samples.

Vickers hardness measurements were performed with a MVK-H0 machine (Akashi Corp). The surfaces were polished before indentation by manual and automatic methods. A force 100 gf was selected for Ti-6Al-4V and a force 300 gf was selected for E-16NiCrMo13. All the measurements were performed according to ASTM E384 standard. A minimum of five indents have been made for each depth. Indent diagonals were measured using a cursor to determine Vickers micro-hardness. Figure 4.7 (a) shows the polishing and hardness indentation locations while Figure 4.7 (b) shows a typical indent for a measurement depth of 50 μm.

(a) Polished surfaces for hardness measurements

(b) Microhardness indent on a Ti-6Al-4V polished surface
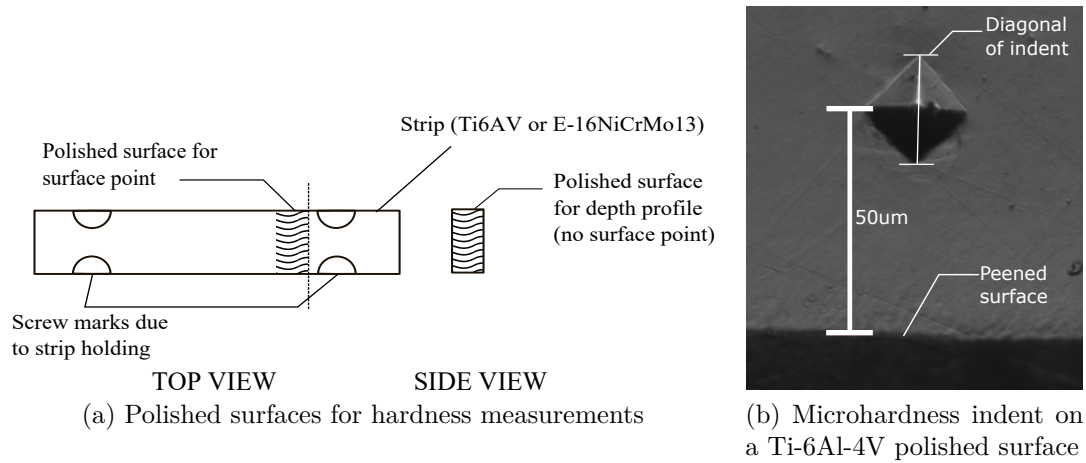
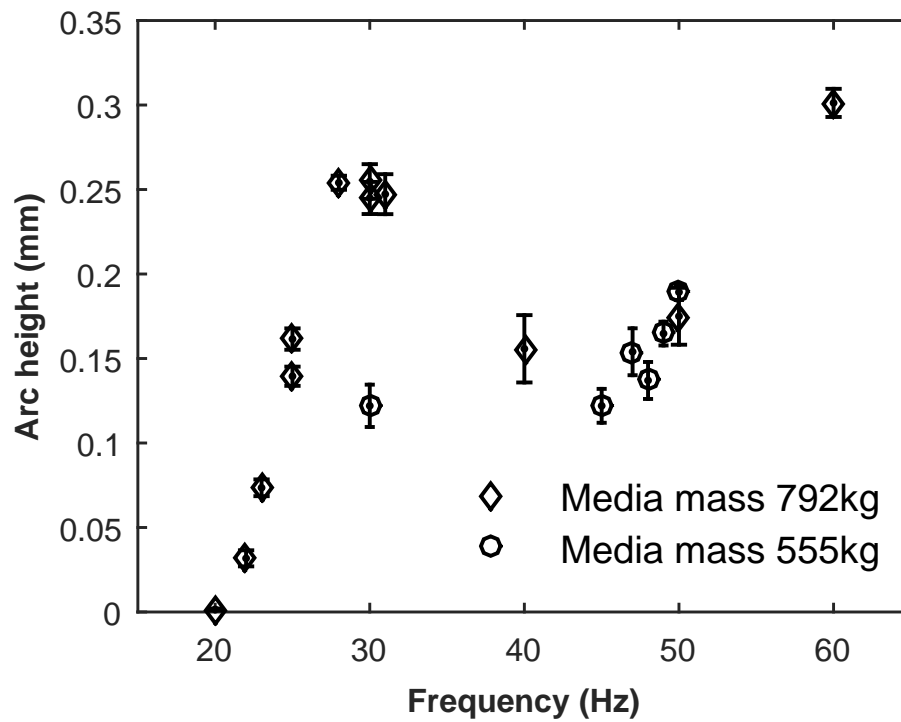Figure 4.7 Microhardness measurements on samples

Figure 4.8 Average arc heights of strips treated with VP process and their 95% confidence intervals as a function of processing frequency for a processing time of 8 minutes and for a four-strips holder depth of 178 mm (the depth is presented on Figure 4.4). The mean and confidence intervals were computed from 4 strips

Table 4.3 Intensity and saturation times (T_{sat}) for the 5 vibratory peening conditions tested

Media mass (kg)	Frequency (Hz)		Position on four-strip holder				Mean	95% confidence
			A	B	C	D		
792	23	Intensity (mmA)	0.11	0.11	0.12	0.12	0.115	0.006
		T_{sat} (min)	20.2	20.2	23.5	25.2	22.3	2.4
792	25	Intensity (mmA)	0.18	0.17	0.18	0.17	0.175	0.006
		T_{sat} (min)	9.7	9.7	7.9	8.6	9.0	0.9
792	30	Intensity (mmA)	0.25	0.25	0.26	0.28	0.26	0.014
		T_{sat} (min)	7.1	7.2	7.6	7.6	7.4	0.3
555	49	Intensity (mmA)	0.21	0.20	0.20	0.22	0.208	0.006
		T_{sat} (min)	15	11	14.2	16.1	14.1	2.1
555	47	Intensity (mmA)	0.18	0.16	0.17	0.20	0.178	0.01
		T_{sat} (min)	13.5	11.1	10.6	12.6	12.0	1.5

4.5 Range of Almen intensities attainable by the selected VP setup studied

The literature suggests that processing time, amplitude, frequency, mass of media, lubrication intensity, position of the part and its orientation in the tub have an influence on the VP process effects. A preliminary study conducted by the authors on Almen strips revealed that processing time, frequency and mass of media were potentially the most influential parameters and were selected for the study.

Figure 4.8 plots the arc height measured on Almen strips vibratory peened for 8 min at different frequencies and for different masses of media. The values are averaged over all the positions on the strips holder, and 95% confidence intervals were computed. Figure 4.8 shows that, for a fixed processing time, the arc height is a non-monotonous function of frequency for a media mass of 792 kg while it is a monotonous function for a media mass of 555 kg. The frequencies of 23 Hz, 25 Hz and 30 Hz and a media mass of 792 kg led to arc heights that could correspond to intensities of 0.12 mmA, 0.18 mmA and 0.25 mmA. Peening frequencies of 47 Hz and 49 Hz, and a media mass of 555 kg, led to arc heights that could correspond Almen intensities of 0.18 mmA. These intensities are representative of peening treatments used in the aerospace industry and were studied further in the sequel.

Table 4.3 lists the variable process parameters along with the calculated intensities and saturation times (T_{sat}). Figure 4.9 shows the relationships between the intensities, frequencies and saturation times, for the two masses of media. Figure 4.9a shows the influence of frequency on the resulting intensity. The figure reveals a strong correlation between the frequency and the resulting intensity, which means that Almen intensity increases with the increase of the frequency. Figure 4.9b shows the influence of frequency on the saturation time. For a mass of media of 792 kg, the saturation time decreased with the increase of frequency. The situation is explained by the fact that a higher frequency led to more impacts per second,

and hence to a faster stabilization of the residual stress field in the strip. However, for a mass of media of 555 kg, this trend seems to be opposite (although not statistically significant). The simultaneous increase of intensity and saturation time could be explained by a higher shot velocity but a lower shot flow rate (impacting mass of media per second) [42]. Figure 4.9c shows the saturation time and intensity relationship for the two studied media masses. The figure shows that there is a significant correlation between the intensity and saturation time for a media mass of 792 kg. This could be a consequence of the shot flow rate being correlated with the shot velocity.

This study reveals that the VP process can consistently deliver Almen intensities in the range of 0.12 mmA to 0.25 mmA.

(a) Intensity as a function of frequency

(b) Saturation time T_{sat} as a function of frequency

(c) Saturation time T_{sat} as a function of intensity
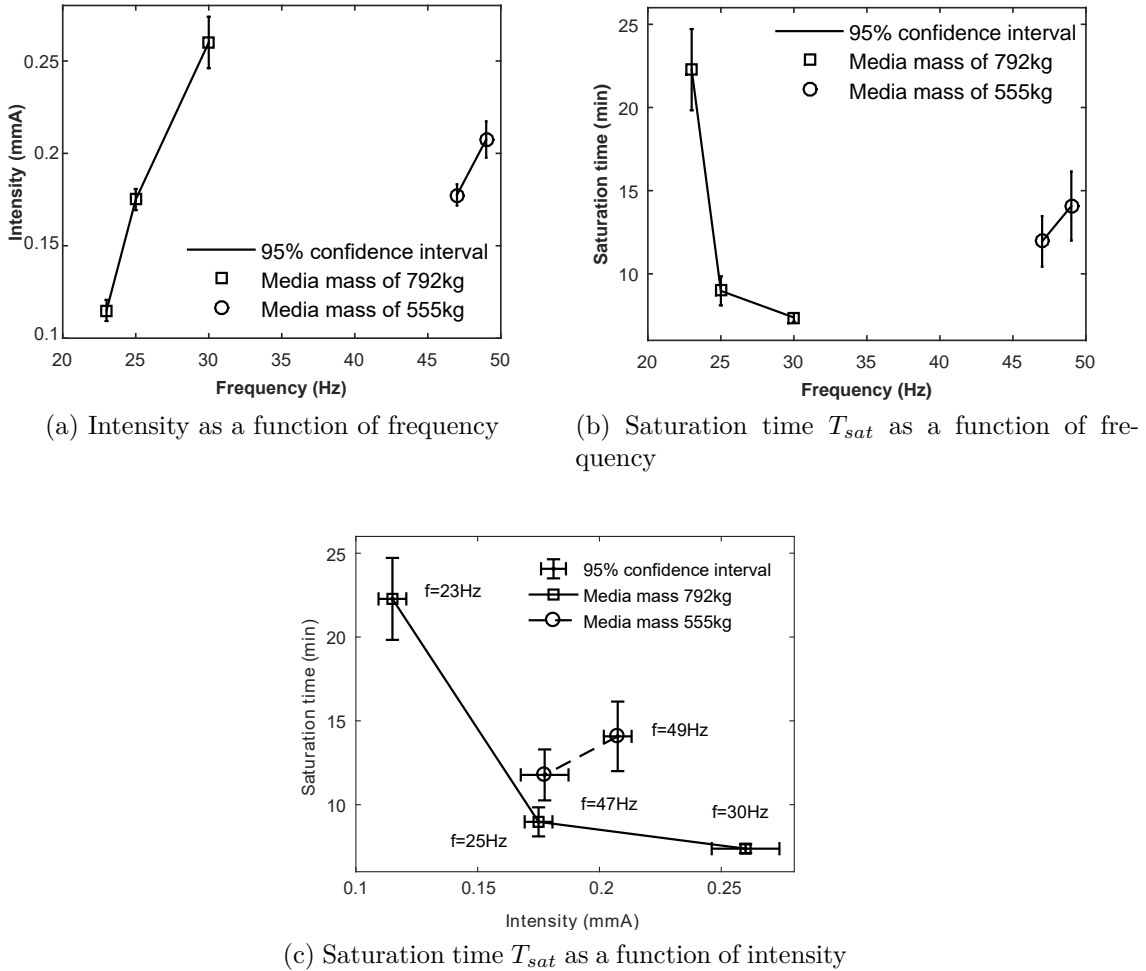
Figure 4.9 Saturation times and intensities with their 95% confidence intervals, for a strip-holder at a processing depth of 178mm (see Figure 4.4) and masses of media of 555 kg and 792 kg

4.6 Effects of vibratory peening on Ti-6Al-4V and E-16NiCrMo13

4.6.1 Processing parameters on Ti-6Al-4V and E-16NiCrMo13 samples

Table 4.4 lists the selected Almen intensity, saturation times, frequency, media mass and the processing times for Ti-6Al-4V samples and E-16NiCrMo13 samples. The processing conditions were the same for the two materials. Three target intensities (0.12, 0.18 and 0.25 mmA) were chosen. The treatment was also applied with different [mass of media - frequency] couples leading to the same Almen intensity of 0.18 mmA to study processing parameters influence on process results. The process was repeated twice for a peening time of T_{sat} to investigate the process' repeatability. Peening times of $T_{sat}/2$, $2T_{sat}$ and $3T_{sat}$ were also investigated on single specimens to investigate the influence of the processing time on the peening results.

Table 4.4 Processing parameters of Ti-6Al-4V and E-16NiCrMo13 samples

Sample number	Intensity/ Saturation time	Frequency (Hz)	Mass of media (kg)	Processing time (normalized/min)	
1	0.12 mmA			T_{sat}	22
2	/	23	792	T_{sat}	22
3	22 min			$2T_{sat}$	44
4	0.18 mmA			T_{sat}	9
5	/	25	792	T_{sat}	9
6	9 min			$2T_{sat}$	18
7	0.25 mmA			T_{sat}	7.5
8	/	30	792	T_{sat}	7.5
9	7.5 min			$2T_{sat}$	15
10				T_{sat}	12
11	0.18 mmA			T_{sat}	12
12	/	47	555	$2T_{sat}$	24
13	12 min			$3T_{sat}$	36
14				$T_{sat}/2$	6
15	Unpeened	/	/	/	/

4.6.2   Results for Ti-6Al-4V

Roughness determination

Figures 4.10a, 4.10b and 4.10c plot roughness parameter R_a as a function of the normalized processing time T_{sat}. These figures shows that the as-machined samples (peening time of 0) exhibited a considerable scatter in Ra. However, the figures suggest that the resulting roughness converges in the range of 0.3 - 0.4 μm. Figure 4.10d plots the average roughness at twice the saturation time as a function of the target intensity. The figure shows that the average roughness increased with the intensity, when the process was applied for $2T_{sat}$. The figure shows that roughness increases linearly with intensity.
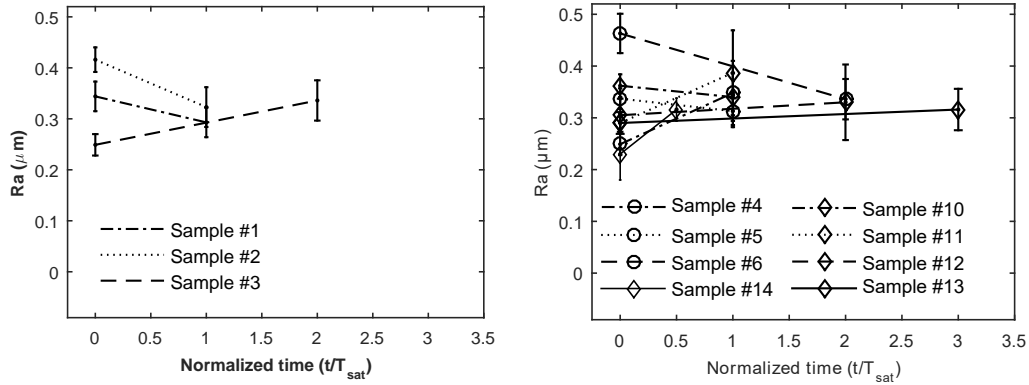
(a) R_a as a function of the normalized time for a peening intensity of 0.12 mmA

(b) R_a as a function of the normalized time for a peening intensity of 0.18 mmA
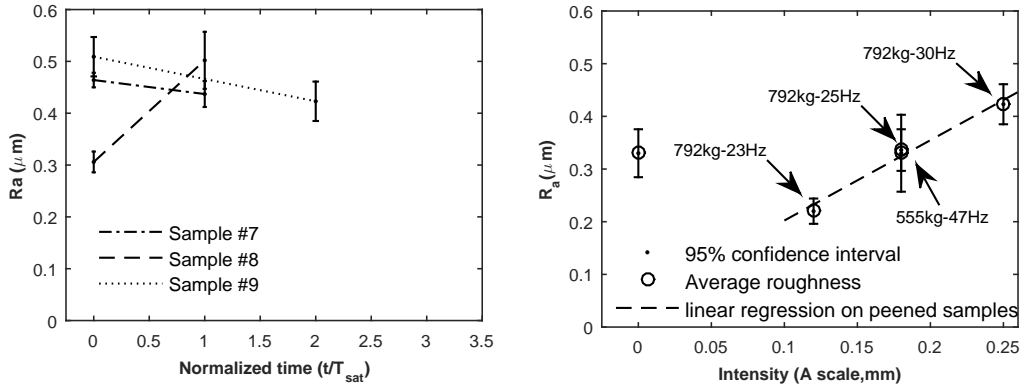
(c) R_a as a function of the normalized time for a peening intensity of 0.25 mmA

(d) R_a as a function of intensity at $2T_{sat}$

Figure 4.10 R_a measurements for Ti-6Al-4V samples, for mass of media-frequency couples of 792 kg-23 Hz(a), 792 kg-25 Hz and 555 kg-47 Hz (b) and 792 kg-30 Hz (c). Subfigure d) plots the averaged Ra as a function of intensity, for a peening time of $2T_{sat}$

Figures 4.11a, 4.11b and 4.11c show 3 typical surfaces unpeened and peened at 0.12 mmA and 0.18 mmA. Figures 4.11b and 4.11c show that machining marks as still visible. However, Figure 4.11b shows that machining marks have been reduced, when compared to the unpeened surface, and that improvement is more significant for the higher peening intensity. On the other hand, Figure 4.11c exhibits more dimples (impact craters) than Figure 4.11b, which is consistent with a higher peening intensity.

Figure 4.12 shows the averaged roughness parameters (R_a, R_{sk}, R_{ku}, RS_m and R_t) over all treated samples before and after vibratory peening. Figure 4.12b suggests that the skewness was globally positive after machining but became negative after vibratory peening. This can result from the fact that the process had flattened the initial peaks. Figure 4.12c shows that R_{ku} oscillates around a value of 4 (when considering the confidence intervals), which correspond to a small number of high peaks and low valleys. Figure 4.12d shows that the process application led to a significant decrease in the spacing parameter RS_m. The fact that the confidence intervals are relatively narrow suggests that the spacing parameter is inherent to the process and independent of frequency and media mass. Figure 4.12 shows that, in overall, the process had a significant impact on R_{sk} and RS_m while little influence for R_a, R_{ku} and R_t.

Residual stress profiles

Figure 4.13 plots the residual stress profiles for different peening intensities for a media mass of 792 kg at twice the saturation time $2T_{sat}$. The unpeened sample exhibits a surface compressive stress of 353 MPa, which is due to the manufacturing process. The figure shows that surface compressive residual stresses are around 600 MPa (the yield strength of Ti-6Al-

(a) Sample #15, unpeened   (b) Sample #3, 0.12 mmA-792 kg, $2T_{sat}$ (c) Sample #13, 0.18 mmA-555 kg, $3T_{sat}$
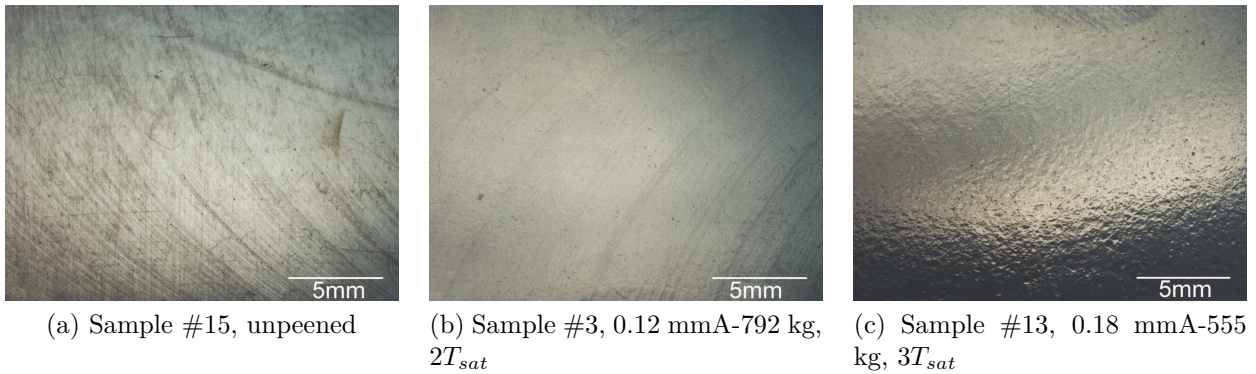
Figure 4.11 (a), (b) and (c) are Ti-6Al-4V surfaces obtained with an optical microscope, magnification 6.7X
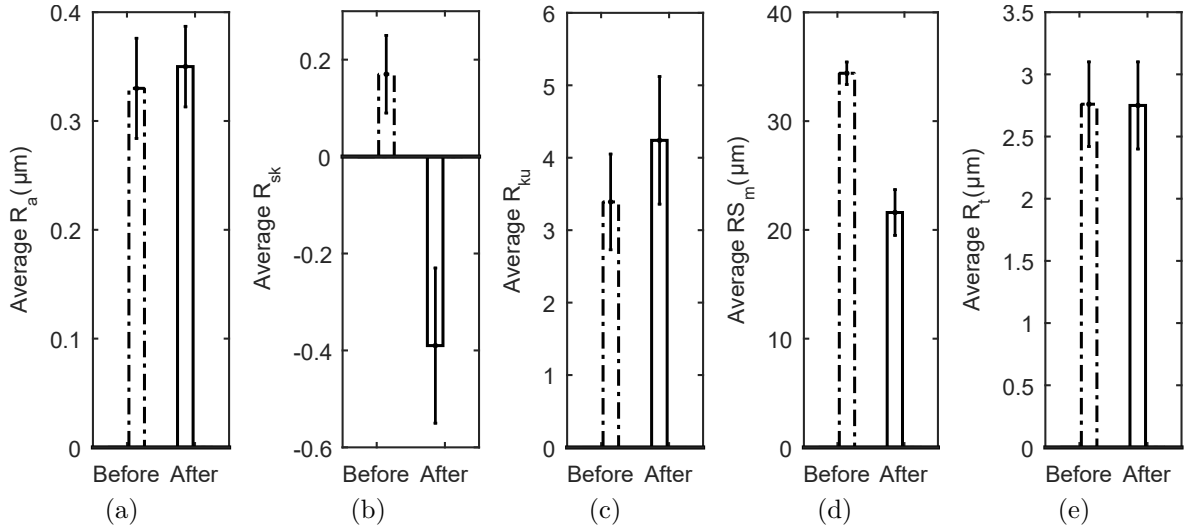
Figure 4.12 Roughness parameters before and after processing for Ti-6Al-4V. R_a (a), R_{sk} (b), R_{ku} (c), RS_m (d), and R_t (e) have been averaged over all samples

4V is of 880 MPa) for the processed samples. Surprisingly, the 0.12 mmA intensity led to the most compressive surface stress, which might be due to the fact that the saturation time is much longer for this lower intensity, as was shown in Figure 4.9c. The figure also shows that the maximum compressive residual stress, as well as the depth at which the profile became positive, increased with the peening intensity.

Figure 4.14 presents the influence of peening media mass and frequency on the residual stresses at twice the saturation time for an intensity of 0.18 mmA. The figure shows that the mass of media and oscillations' frequency have an influence on the residual stress profile since peening with 555 kg of media at a frequency of 47 Hz for 22 minutes led to more compressive and deeper stresses than peening with 792 kg of media at a frequency of 25 Hz for 18 minutes. This difference might result from the higher frequency, which led to more impacts, for a media mass on 555 kg. This situation would tend to make the treated material reach a stabilized plastic behavior faster for the higher treatment frequency.

Figure 4.15 compares the influence of peening time on the residual stress profiles for a tub filled with 555 kg of media and oscillating at 47 Hz. The figure shows that increasing the peening time to twice the saturation time increased the compressive stresses and their depth. However, peening at three times the saturation time did not alter further the residual stress profile. This observation supports the above-mentioned hypothesis that peening time could significantly influence the residual stresses.
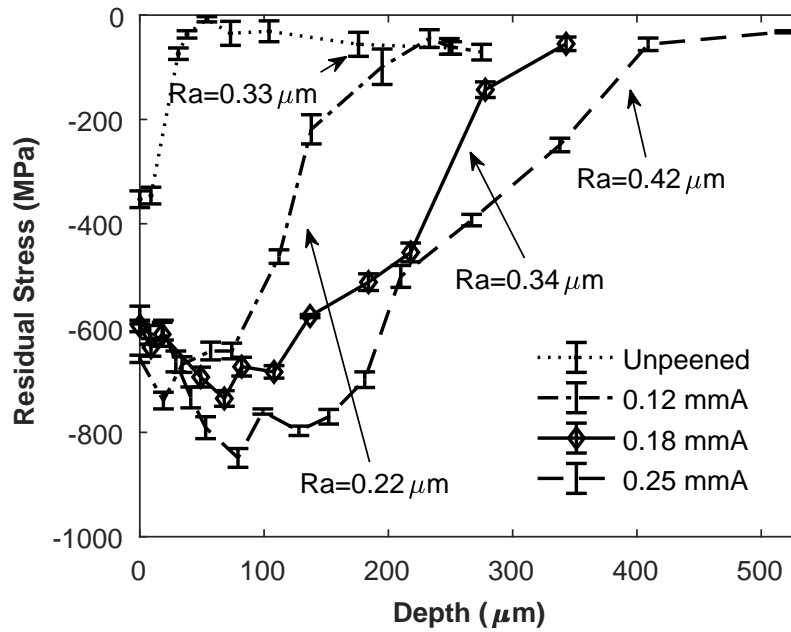
Figure 4.13 Residual stress profiles for different peening intensities for Ti-6Al-4V (792 kg of media, processing time of $2T_{sat}$)
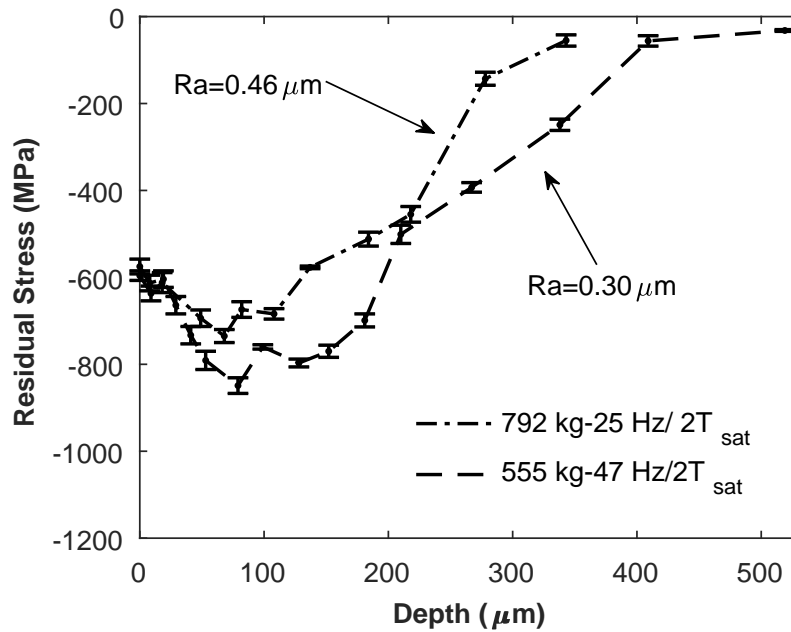
Figure 4.14 Residual stress profiles for Ti-6Al-4V samples peened at 0.18 mmA for media mass-frequency couples of 792 kg-25 Hz and 555 kg-47 Hz
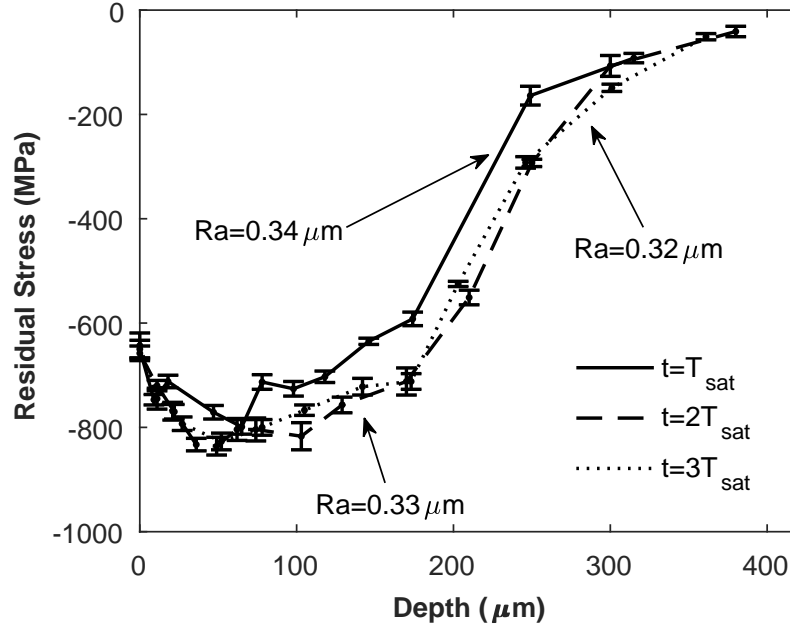
Figure 4.15 Residual stress profiles for Ti-6Al-4V peened at 0.18 mmA for different processing times (12, 24 and 36 minutes) for media mass-frequency couples of 555 kg-47 Hz

Hardness profiles

Figure 4.16 shows hardness profiles for Ti-6Al-4V samples peened at three different intensities for a media mass of 792 kg and a saturation time T_{sat}. The figure reveals that vibratory peening induces hardness increase only within the first 60 μm below the surface. The surface hardness measurements (with 95% confidence intervals) for different peening conditions are presented in Figure 4.17. It can be seen that, when compared to the unpeened sample, vibratory peening increased the hardness of the treated samples in the range of +8.2% for sample # 13 and +15.5% for sample # 4. However, the 95% confidence intervals exhibit significant scatter, which prevents statistically significant observations to be made regarding machine parameters influence on hardness.

Comparison with shot peening

Table 4.5 presents a comparison of resulting average roughness of shot peening and vibratory peening processes. For both Almen intensities (0.12 mA and 0.18 mmA), R_a parameters is about -80% lower after vibratory peening process, when compared with shot peening.

Table 4.6 summarizes the key values of the residual stresses profiles of Ti-6Al-4V samples submitted to vibratory peening and conventional shot peening at similar intensities while
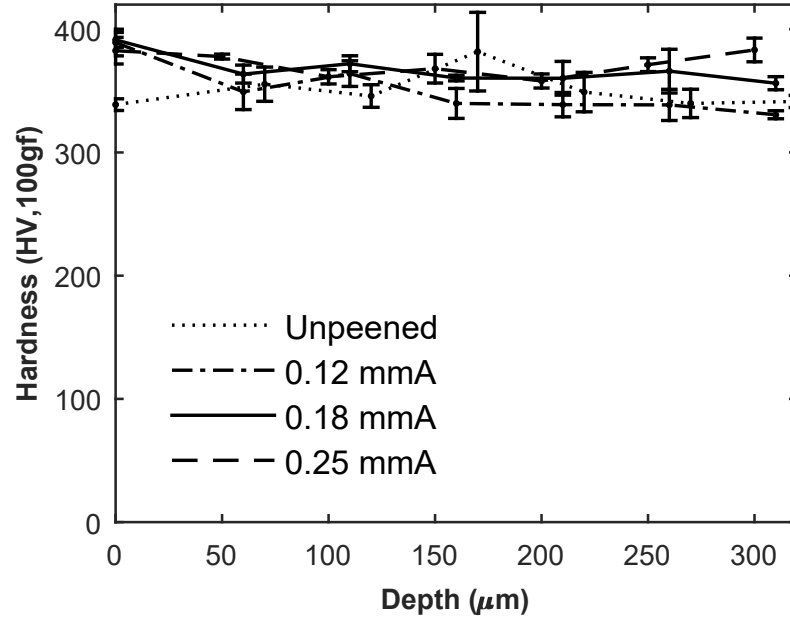
Figure 4.16 Hardness profiles measured on the cross-section for Ti-6Al-4V samples peened at different intensities and for a mass of media and peening time of 792 kg and T_{sat}
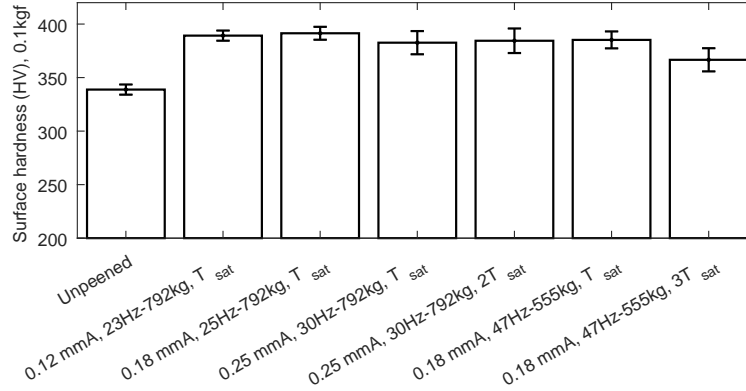
Figure 4.17 Surface hardness measurements and their 95% confidence intervals for Ti-6Al-4V samples for different peening conditions

Figure 4.18 plots the residual stress profiles corresponding to these samples. The table shows that the values of surface residual stresses and maximum compressive residual stresses are quite similar for both processes, for each comparable Almen intensity (0.12 mmA and 0.18 mmA). The position of the peak of compressive stress is also similar for both processes. However, the width of material impacted by the processes seems to be more important for vibratory peening, when compared to shot peening and extrapolating the stress profiles. It

Table 4.5 Comparison of surface roughness R_a (μm) for different intensities between vibratory peening (samples # 3 and # 6) and shot peening, for Ti-6Al-4V

	0.12 mmA	0.18 mmA
Shot peening	1.10	1.85
Vibratory peening	0.22	0.34
Difference	-80%	-82%

Table 4.6 Comparison of residual stresses for different intensities between vibratory peening (samples # 3 and # 6) and shot peening, for Ti-6Al-4V

Parameter	0.12 mmA			0.18 mmA		
	SP	VP	Difference	SP	VP	Difference
σ_{surf} (MPa)	-670	-659	-2%	-590	-596	1%
σ_{max} (MPa)	-700	-739	6%	-730	-735	1%
$Z_{\sigma_{max}}$ (μm)	40	19	-53%	68	68	0%
Profile depth (μm)	/	220	/	/	343	/
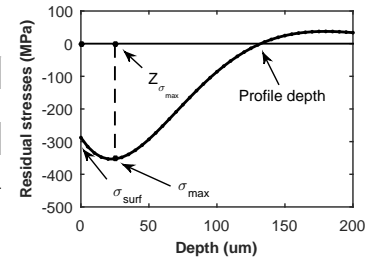
Figure 4.18 Comparison of shot peening induced and vibratory peening induced residual stress profiles of Ti-6Al-4V samples treated at 0.12 and 0.18 mmA

seems that the vibratory peening process at an intensity of 0.12 mmA induces equivalent residual stresses to the shot peening process at an intensity of 0.18 mmA. It appears, using Table 4.5, that for similar residual stresses, vibratory peening resulted in a low surface

roughness, when compared to shot peening (-88%).

4.6.3 Results for E-16NiCrMo13

Roughness determination

Figure 4.19a, Figure 4.19b and Figure 4.19c present the average roughness R_a evolution as a function of the processing time for different process conditions on steel E-16NiCrMo13. The figures show that roughness decreased with the increase of the peening time and stabilized at around 0.4 μm at twice the saturation time $2T_{sat}$ for the different processing conditions. Moreover, increasing the peening time decreased the results scatter. Figure 4.19d plots R_a
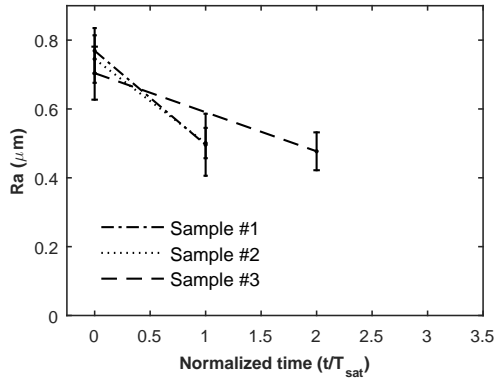
(a) R_a as a function of the normalized time for a peening intensity of 0.12 mmA
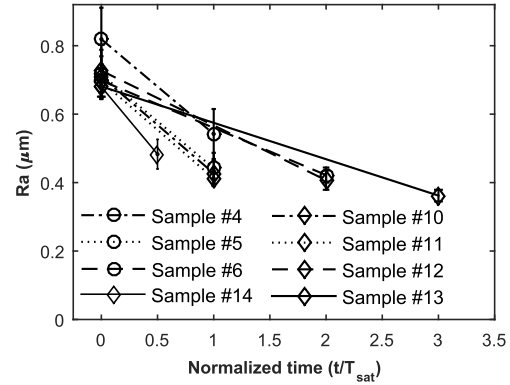
(b) R_a as a function of the normalized time for a peening intensity of 0.18 mmA
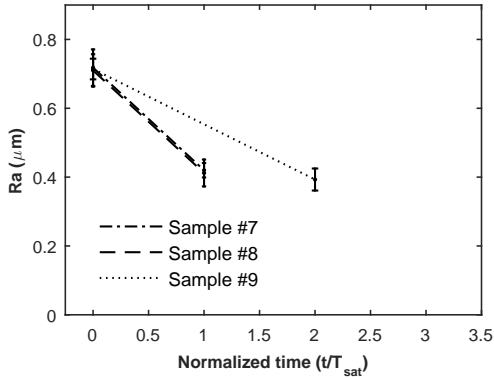
(c) R_a as a function of the normalized time for a peening intensity of 0.25 mmA
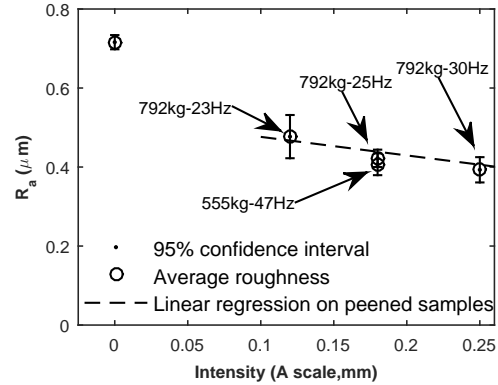
(d) R_a as a function of intensity at $2T_{sat}$

Figure 4.19 R_a measurements for E-16NiCrMo13 samples, for mass of media-frequency couples of 792 kg-23 Hz(a), 792 kg-25 Hz and 555 kg-47 Hz (b) and 792 kg-30 Hz (c). Subfigure d) plots the averaged R_a as a function of intensity, for a peening time of $2T_{sat}$. An intensity of 0 corresponds to the unpeened specimen

parameter at twice the saturation time as a function of target intensity. The figure shows that peening intensity has an insignificant impact on surface roughness after twice the saturation time $2T_{sat}$.

Figure 4.20 shows three typical surfaces of unpeened sample (4.20a) and samples vibratory peened at intensities of 0.12 mmA (4.20b) and 0.18 mmA (Figure 4.20c). These pictures were taken by an optical microscope at a magnification of 6.7X. Figures 4.20b and 4.20c show that machining marks are still visible, when compared to the unpeened surface. However, these marks are shinier on Figure 4.20c and dimples can be observed on Figure 4.20c, which is due to the fact that the peening intensity in Figure 4.20c was higher than that in Figure 4.20b.

Figure 4.21 shows the averaged roughness parameters (R_a, R_{sk}, R_{ku}, RS_m and R_t) over all treated samples before and after vibratory peening. The figure shows how the process statistically affected all these parameters. Figure 4.21b shows that skewness is negative after and before peening, which means that samples surface profiles exhibit more valleys than peaks. A decrease in the skewness after peening means that peaks have been flattened by the media. Figure 4.21c shows that kurtosis remained relatively constant. The average value of 4.3 suggests that the surface is quite flat with dispersed peaks and valleys. A decrease of RS_m parameter is observed after peening (Figure 4.21d). R_t (Figure 4.21e) seems to go through the same changes as R_a. The maximum peak to valley height is reduced significantly after peening, which further supports the fact that peaks have been rounded. This result is interesting for such a material when used in parts where contacts are important, as in gears for example.

(a) Sample #15, unpeened   (b) Sample #3, 0.12 mmA-792 kg,   (c) Sample #13, 0.18 mmA-555
                                $2T_{sat}$ kg, $3T_{sat}$
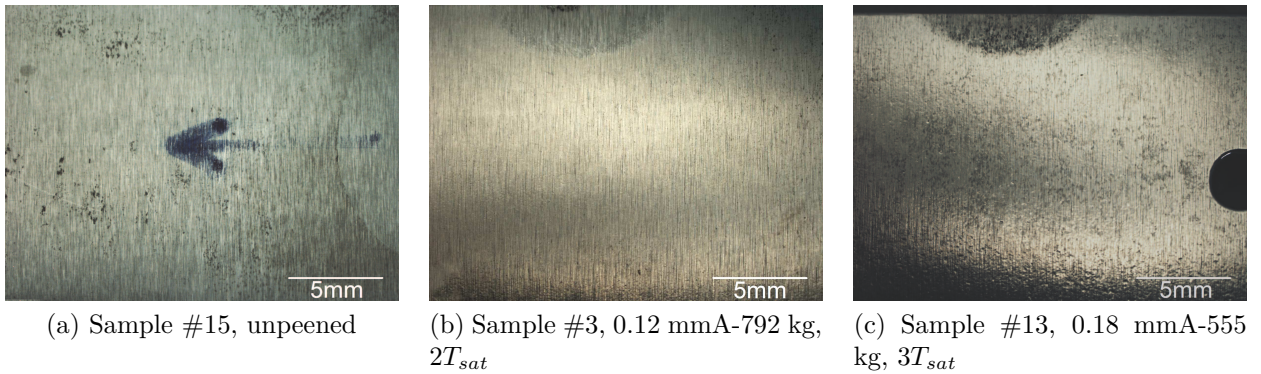
Figure 4.20 (a), (b) and (c) are E-16NiCrMo13 surfaces obtained with an optical microscope, magnification 6.7X
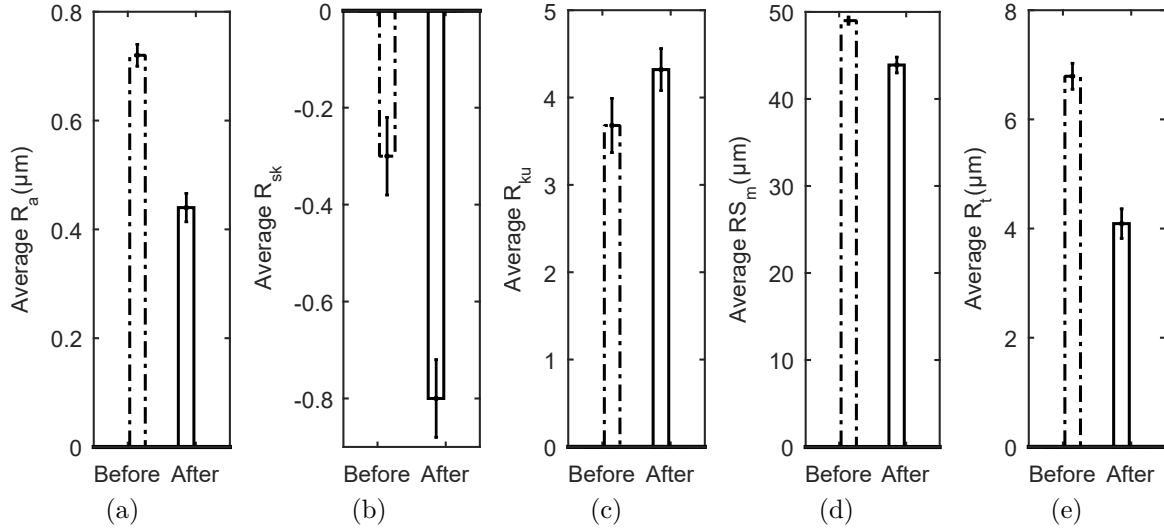
Figure 4.21 Roughness parameters before and after processing for E-16NiCrMo13. R_a (a) value is the mean of samples' R_a peened at $t \geq 2T_{sat}$, R_{sk} (b), R_{ku} (c), RS_m (d), and R_t (d) have been averaged over all samples

Residual stress profiles

Figure 4.22 compares the effects of peening intensity on residual stresses for E-16NiCrMo13 at twice the saturation peening time. As it was observed for Ti-6Al-4V, it seems that peening at an intensity of 0.12 mmA leads to more surface compressive residual stresses than peening at the other higher intensities. Similarly to Ti-6Al-4V, the maximum compressive residual stresses, as well as the depth where the residual stress seems to reach a plateau, increased with the peening intensity. Figure 4.22 reveals the influence of case hardening on the residual stress field. The unpeened sample had a null surface residual stress but compressive stresses built up to 200 MPa and stabilized at a depth of 100 μm. It can be seen that the peening induced stresses stabilized to that value down to 400 μm. Extracting residual stresses deeper in the material is required to determine the position at which residual stresses become tensile to balance these compressive stresses.

Figure 4.23 compares two residual stress profiles from samples peened at 0.18 mmA for different mass of media and frequency couples. The same tendency as that observed for Ti-6Al-4V can be observed: increasing the peening time has an influence on the residual stress profile. Figure 4.24 further shows the influence of processing time on residual stress profiles for a peening intensity of 0.18 mmA and a media mass of 555 kg. The figure shows that, when the peening time increases from T_{sat} to $2T_{sat}$, the residual stress profile becomes more compressive and deeper. When the peening time increases from $2T_{sat}$ to $3T_{sat}$, the

compressive residual stress profile reaches a plateau.
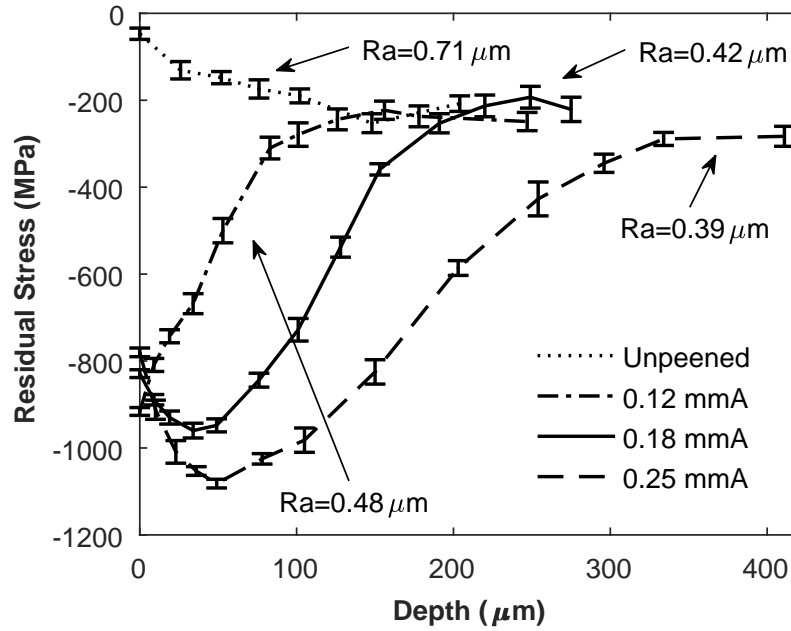
Figure 4.22 Residual stress profiles for different peening intensities for E-16NiCrMo13 (792 kg of media, $2T_{sat}$)
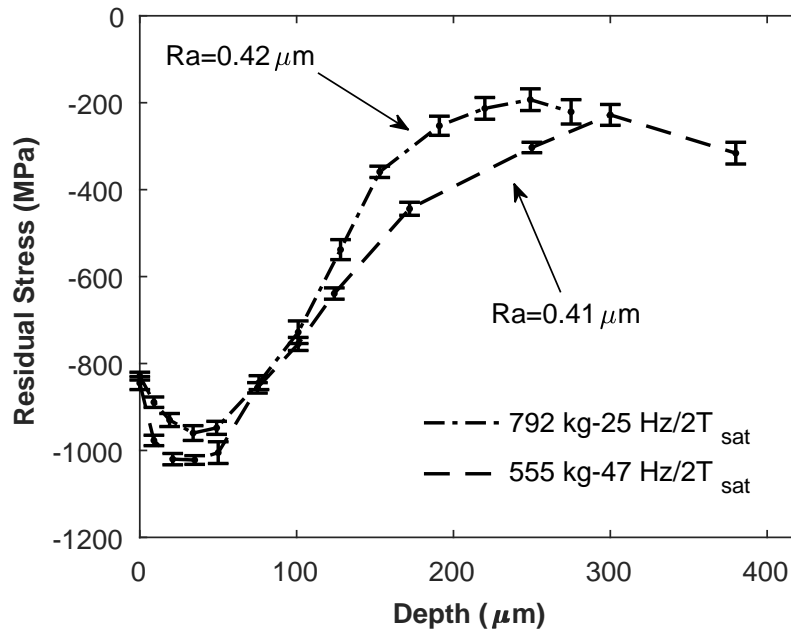
Figure 4.23 Residual stress profiles for E-16NiCrMo13 samples peened at 0.18 mmA for media mass-frequency couples of 792 kg-25 Hz and 555 kg-47 Hz

Hardness profiles

Figure 4.25 compares the hardness profiles for E-16NiCrMo13 samples peened for three different intensities and for a mass of media and peening time of 792 kg and T_{sat}. It can be seen that vibratory peening slightly increases the hardness profile (around 10%) within the first 70 μm. Figure 4.26 shows the surface hardness measurements for different peening conditions. A significant hardness increase due to peening in the range of +8.3% with sample # 4 to +13.8% with sample # 13 can be observed. The surface hardness values are very similar for the three different intensities (0.12 mmA, 0.18 mmA and 0.25mmA) at saturation time. It should be noted that saturation time differs for different intensities. For example, the peening time of sample 0.12 mmA-T_{sat} is almost three times that of sample 0.25 mmA-T_{sat}.

Comparison with shot peening

Table 4.7 presents a comparison of resulting average roughness of shot peening and vibratory peening processes. For an Almen intensity of 0.12 mmA, R_a parameters is about -32% lower after vibratory peening process, when compared with shot peening. The difference is even higher for 0.18 mmA Almen intensity, where average roughness of vibratory peened sample is -40% lower, when compared to shot peened sample.
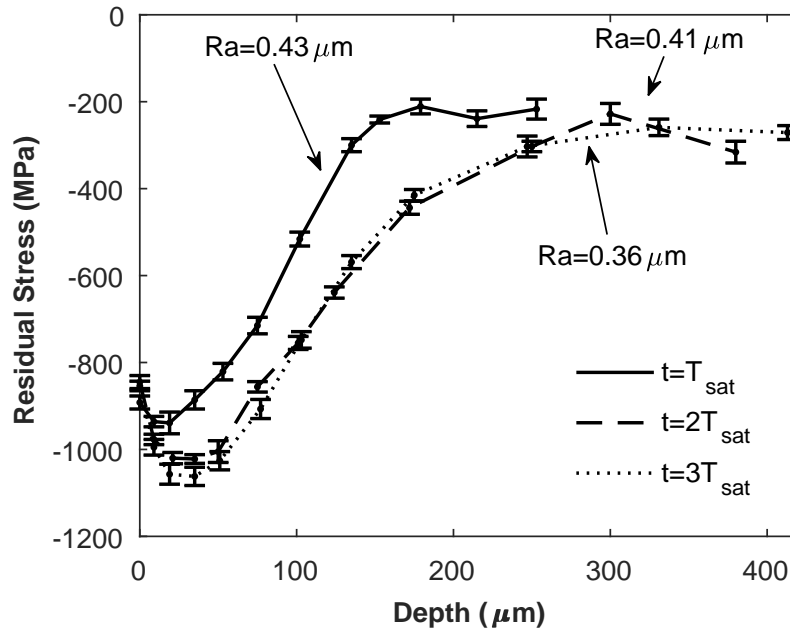
Figure 4.24 Residual stress profiles for E-16NiCrMo13 peened at 0.18 mmA for different processing times (T_{sat}, $2T_{sat}$ and $3T_{sat}$) for media mass-frequency couples of 555 kg-47 Hz
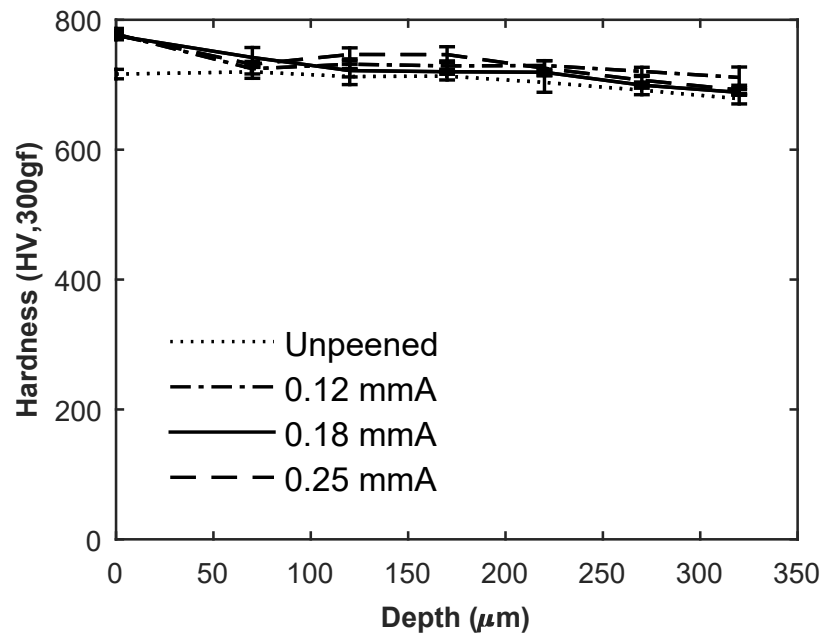
Figure 4.25 Hardness profiles measured on the cross-section for E-16NiCrMo13 samples peened at different intensities and for a mass of media and peening time of 792 kg and T_{sat}
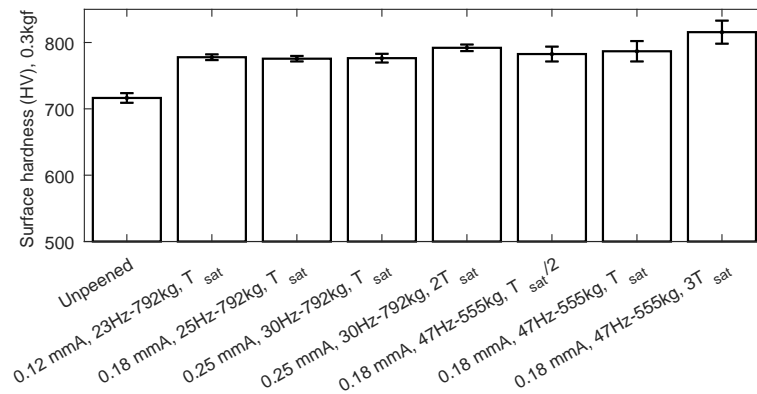
Figure 4.26 Surface hardness measurements and their 95% confidence intervals for E-16NiCrMo13 samples for different peening conditions

Table 4.8 summarizes the key values of the residual stresses profiles of E-16NiCrMo13 samples submitted to vibratory peening and conventional shot peening at similar intensities and Figure 4.27 shows the compressive residual stress profiles with depth. The table shows that vibratory peening appears to induce higher surface residual stresses (+50% at 0.12 mmA and +24% at 0.18 mmA), when compared to shot peening. Similarly, the values of

Table 4.7 Comparison of surface roughness R_a (μm) for different intensities between vibratory peening (samples # 3 and # 6) and shot peening, for E-16NiCrMo13

	0.12 mmA	0.18 mmA
Shot peening	0.71	0.70
Vibratory peening	0.48	0.42
Difference	-32%	-40%

Table 4.8 Comparison of residual stresses for different intensities between vibratory peening and shot peening, for E-16NiCrMo13

Parameter	12 mmA			18 mmA		
	SP	VP	Difference	SP	VP	Difference
σ_{surf}(MPa)	-610	-916	50%	-670	-829	24%
σ_{max}(MPa)	-610	-916	50%	-750	-960	28%
$Z_{\sigma_{max}}$(μm)	0	0	0%	23	34	48%
Profile depth (μm)	70	155	121%	95	220	131%
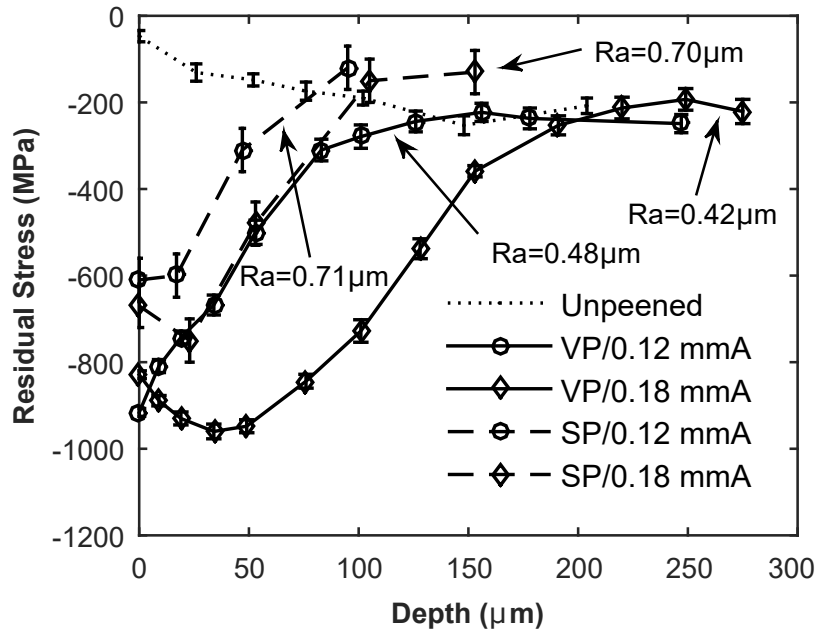
Figure 4.27 Comparison of shot peening induced and vibratory peening induced residual stress profiles of Ti-6Al-4V samples treated at 0.12 and 0.18 mmA

the maximum of compressive residual stresses are higher with vibratory peening (+50% at 0.12 mmA and +28% at 0.18 mmA), when compared to shot peening. The maximum of compressive stresses is situated on surface for specimen peened at 0.12 mmA intensity with

both processes. The peak of compressive stresses is deeper for vibratory peening when peened at 0.18 mmA (+48%), when compared to shot peening. The width of the impacted residual stresses layer is more important for vibratory peening (+126% in average), when compared to shot peening.

4.7 Discussion

4.7.1 Roughness

Figure 4.12 and Figure 4.21 show that the vibratory peening process modified R_{sk} and R_{ku} values for the two studied materials. These figures also show that Ti-6Al-4V average roughness R_a was stable around 0.33 ± 0.06 μm and E-16NiCrMo13 converged to an average R_a of 0.41 ± 0.02 μm. Althought the hardness values are significantly different for these materials, prior to and after the treatment, the converged values for roughness remain in the same range for both materials. This observation is consistent with Hashimoto's model [30] which suggests that roughness converges to a value that depends only on the process. Further analysis is required to confirm this trend since Wang et al. [33] and Baghbanan et al. [20] exposed two different aluminum alloys to vibratory finishing and obtained different roughness results.

The spacing roughness parameter RS_m after peening with the same peening parameters were 21 μm and 45 μm for Ti-6Al-4V and E-16NiCrMo13, respectively. Comparison with the initial value of 35 μm for Ti-6Al-4V shows that peening erased the milling marks. However, the initial RS_m for E-16NiCrMo13 was of 49 μm, which shows that the peening process had little influence on this parameter. This could be explained by the much higher surface hardness of E-16NiCrMo13 (720 HV), when compared to that of Ti-6Al-4V (340 HV). In addition, the media had a hardness of 740 HV, which is quite close to that of the treated steel.

Observation of the vibratory peened surface (Figures 4.11 and 4.20) revealed that the impact imprints were spherically shaped, which is due to the fact that the media flow was orthogonal to the peened surface. Tilting the sample with respect to the media flow could increase the finishing effect and thus remove the machining marks, as it was osberved by Sangid et al. [22]. Further investigation is required to confirm that hypothesis.

4.7.2 Residual stresses

The comparison of Table 4.6 and Table 4.8 reveals that the influence of vibratory peening on residual stresses profiles follow the same trends for both materials. When the peening

intensity increases, the maximum compressive residual stress and the depth of the compressive region increase. In conclusion, these observations suggest that vibratory peening and shot peening lead to similar effects on surface stresses. However, vibratory peening led to deeper compressive residual stresses and produced larger maximum compressive residual stresses, when compared with shot peening.

Figure 4.15 and Figure 4.24 revealed that the residual stress profiles saturated for the same normalized time $2T_{sat}$ for a peening intensity of 0.18 mmA (555 kg of media and oscillating at 47 Hz) for both materials. Additional studies are required to investigate if the same trend would be observed for different machine parameters.

4.7.3   Hardness

For both studied materials, vibratory peening increased only surface hardness down to a depth of 60 μm for Ti-6Al-4V and 70 μm for E-16NiCrMo13. When all the measurements are averaged, surface hardness increased by 45 ± 9 HV for Ti-6Al-4V (from 339 HV to 384 HV) and 61 ± 14 HV for E-16NiCrMo13 (from 716 HV to 778 HV) from the unpeened to the peened samples. However, no direct relation between process parameters and surface hardness have been drawn.

4.7.4   Comparison with conventional shot peening

Some extra samples have been shot peened at intensities of 0.12 mmA and 0.18 mmA for both materials for comparison purposes. The surfaces' roughness have been recorded, and it can ben noted that R_a parameter is lower with the vibratory peening process for both materials, when compared with the shot peening process. Differences of -81% for titanium and -36% for steel have been measured with VP, when compared to SP. The VP process induced surface and maximum compressive stresses equal to shot peening on titanium for both intensities but more important than shot peening (+50% at 0.12 mmA and about +25% at 0.18 mmA) on steel samples. Globally, the position of the maximum compressive stress of the profile is identical for both processes, expect for the steel sample treated at an intensity of 0.18 mmA, where the position of the maximum was found to be deeper for vibratory peening, when compared to shot peening. The depth of the profile was more important for vibratory peening, when compared to shot peening for both materials (depth increase of +126% with E-16NiCrMo13, unknown for Ti-6Al-4V).

4.8 Conclusion

This study revealed that:

- Vibratory peening can consistently deliver peening intensities in the range of 0.12 mmA to 0.25 mmA, as in conventional shot peening, thus making the Almen intensity an appropriate parameter to specify vibratory peening.

- Milling marks on Ti-6Al-4V specimens have been erased but average roughness R_a did not change. The manufacturing marks on E-16NiCrMo13 sample could not be removed by vibratory peening, but have been smoothened. The roughness R_a of both materials reduced to 0.3-0.4 μm after vibratory peening, independently on the peening parameters. Surface coverage, as defined in shot peening, could not be used for vibratory peening.

- Maximum compressive stress and depth increased with the increase of vibratory peening intensity. Residual stress profiles saturated for both materials after a certain peening time (for example, $2T_{sat}$ for 555 kg of media and frequency of 47 Hz).

- When compared to conventional shot peening, the surface and maximum compressive residual stresses from VP are equal in magnitude and deeper for Ti-6Al-4V. When compared to conventional shot peening, the surface and maximum compressive residual stresses from VP are higher in magnitude and deeper for E-16NiCrMo13.

- Vibratory peening had low effect on the hardness for both materials within a depth of 70 μm. There is no significant hardness variation through the different processing conditions.

In conclusion, the VP seems to induce the same beneficial effects as shot peening (compressive residual stresses) for a much better surface finish. These observations suggests that VP should deliver fatigue life improvement, the magnitude of which will be studied in a follow-up research.

Aknowledgements

CHAPTER 5   GENERAL DISCUSSION

The experiments covered three machine parameters, namely frequency of vibrations, mass of media and processing time. The low number of samples and the allotted time to the experiments limited this study and prevented to investigate other processing parameters. The orientation of the part is expected to have a significant influence on the resulting fatigue life, roughness and residual stresses as reported by Sangid et al. [22]. The authors showed that the fatigue life enhancement performance was a trade-off between the roughness improvements and the compressive residual stresses intensity, and that changing the orientation of the part could decrease the roughness while decreasing the residual stresses. The authors also showed that the position of the part within the tub had also a significant influence on results. The machine they used had a circular movement. On the opposite, the VP machine used in this study have a up and down movement. Therefore the position of the part within the tub should not be significant on the results with this machine.

The standardized Almen intensity system has been used with the VP process. The study is bounded by the 0.12 mmA and 0.25 mmA intensities. Therefore the results exposed by the present thesis are valid in this range of intensities. As the vibrations frequency and the mass of media varied in limited ranges, respectively [0 Hz - 47 Hz] and [555 kg - 792 kg], extending these ranges could allowed the process to reach a wider range of intensities.

The study of the VP process effects presented here covers two aerospace materials, namely E-16NiCrMo13 and Ti-6Al-4V. Therefore, the validity of the conclusions is restricted to these two materials and can not be extended to other materials without further investigations.

For funding and time purpose, no fatigue tests were performed in this study. Therefore the beneficial effect of the VP on the fatigue lives of components is purely hypothetical and should be investigated in the upcoming studies.

CHAPTER 6   CONCLUSION AND RECOMMENDATIONS

The effects of the vibratory peening process in terms of roughness, hardness and residual stresses have been investigated and compared to those of the shot peening process, for comparable Almen intensities.

This research revealed that vibratory peening delivers Almen intensities in the range of 0.12 mmA - 0.25 mmA, consistently.
Samples made of Ti-6Al-4V and E-16NiCrMo13 were submitted to the vibratory peening process for different Almen intensities. The process impacted the surface finish of both materials, erasing the milling marks of Ti-6Al-4V and smoothing the rectification marks of E-16NiCrMo13. The average roughness parameter remained in a similar range of values (0.3-0.4 μm) for titanium as it was originally low before processing. This parameter decreased on E-16NiCrMo13 samples and converged to 0.4 μm, regardless the processing parameters. The process induced significant residual stresses in a sub-surface layer. The value of maximum compressive stress and its depth increased with the Almen intensity, as the width of the impacted layer. Processing time appeared to have the very same influence on residual stress profiles but seemed to show a saturation in the effects after a processing time of $2T_{sat}$ for the [555 kg- 47 Hz] condition. The samples hardness was affected by the process in a layer of 70 μm. However, no trends could be drawn regarding the effects of processing parameters on hardness.

The effects of the vibratory peening process have been compared to those of the shot peening process in terms of residual stresses and roughness. The comparison has been made for Almen intensities of 0.12 mmA and 0.18 mmA and revealed that vibratory peening globally led to deeper compressive residual stresses (no quantitative data for Ti-6Al-4V, +126% for E-16NiCrMo13), with a higher magnitude (similar for Ti-6Al-4V, +38% in average for E-16NiCrMo13). The vibratory peening process led to lower roughness, when compared to the shot peening process (about -81% for Ti-6Al-4V and -36% for E-16NiCrMo13).

In conclusion, this study showed that VP delivers better surface finish as well as deeper and more compressive residual stresses than shot peening, for the same Almen intensity. This observation suggests that VP could deliver equal or higher fatigue lives than shot peening and could be used for both peening and surface finishing, in a single step.

Future works

The research work concluded that the VP has the potential to improve the fatigue lives of components. The next step is to confirm that conclusion by performing fatigue life tests on vibratory peened and shot peened parts and compare them.

The investigation of the orientation of the part within the machine could lead to an optimal trade-off between the surface roughness and the residual stresses.

The vibratory peening process is a complex surface treatment that would require a sound scientific investigation to demonstrate the fluidized media mechanics. The media flow in the tub is highly dependent of the machine's shape and the operation parameters. Future works should focus on investigating the media flow within the tub and develop predictive models. These models could be used to optimize the process parameters.

BIBLIOGRAPHY

[1] D. A. Davidson, "Mass finishing processes," *Metal finishing*, vol. 100, pp. 104–117, 2002.

[2] E. Holzknecht, "Everything you need to know about mechanical/mass finishing: A workshop on the role of media in mechanical surface finishing," *Metal Finishing*, vol. 107, no. 5, pp. 27–31, 2009.

[3] G. Feldmann, C. C. Wong, W. Wei, and T. Haubold, "Application of Vibropeening on Aero–Engine Component," *Procedia CIRP*, vol. 13, pp. 423–428, 2014.

[4] J. Solis Romero, A. Anguiano García, and A. García Macedo, "Surface roughness and residual stresses on the fatigue life of shot peened components: Theoretical determination," *Ingeniería mecánica, tecnología y desarrollo*, vol. 3, no. 1, pp. 17–20, 2008.

[5] S. Gangaraj and G. Farrahi, "Side effects of shot peening on fatigue crack initiation life," *International Journal of Engineering-Transactions A: Basics*, vol. 24, no. 3, p. 275, 2011.

[6] A. Inoue, T. Sekigawa, and K. Oguri, "Fatigue property enhancement by fine particle shot peening for aircraft aluminum parts," in *Conf Proc: ICSP-10, Tokyo, Japan*, 2008.

[7] A. Tange and K. Ando, "Improvement of spring fatigue strength by new warm stress double shot peening process," *Materials science and technology*, vol. 18, no. 6, pp. 642–648, 2002.

[8] SAE International, "Procedures for Using Standard Shot Peening Test Strip, J443," 2017.

[9] ——, "Test Strip, Holder, and Gage for Shot Peening, J442," 2017.

[10] ——, "Shot Peening Coverage Determination, J2277," 2013.

[11] Z. Liu, T. Wong, W. Huang, N. Sridhar, and S. Wang, "Effect of Surface Polishing Treatment on the Fatigue Performance of Shot-Peened Ti–6Al–4V Alloy," *Acta Metallurgica Sinica (English Letters)*, pp. 1–11, 2017.

[12] L. Xie, Y. Wen, K. Zhan, L. Wang, C. Jiang, and V. Ji, "Characterization on surface mechanical properties of Ti–6Al–4V after shot peening," *Journal of Alloys and Compounds*, vol. 666, pp. 65–70, 2016.

[13] R. Mediratta, K. Ahluwalia, and S. Yeo, "State-of-the-art on vibratory finishing in the aviation industry: an industrial and academic perspective," *The International Journal of Advanced Manufacturing Technology*, vol. 85, no. 1-4, pp. 415–429, 2016.

[14] D. Semones and W. Safranek, "Chemically accelerated metal finishing process," Sep. 14 1976, uS Patent 3,979,858. [Online]. Available: http://www.google.ch/patents/US3979858

[15] D. Bańkowski and S. Spadło, "Investigations of influence of vibration smoothing conditions of geometrical structure on machined surfaces," in *IOP Conference Series: Materials Science and Engineering*, vol. 179, no. 1.   IOP Publishing, 2017, p. 012002.

[16] F. Hashimoto and S. P. Johnson, "Modeling of vibratory finishing machines," *CIRP Annals-Manufacturing Technology*, vol. 64, no. 1, pp. 345–348, 2015.

[17] S. E. Naeini and J. Spelt, "Two-dimensional discrete element modeling of a spherical steel media in a vibrating bed," *Powder Technology*, vol. 195, no. 2, pp. 83–90, 2009.

[18] S. Naeini and J. Spelt, "Development of single-cell bulk circulation in granular media in a vibrating bed," *Powder technology*, vol. 211, no. 1, pp. 176–186, 2011.

[19] K. Hashemnia and J. K. Spelt, "Finite element continuum modeling of vibrationally-fluidized granular flows," *Chemical Engineering Science*, vol. 129, pp. 91–105, 2015.

[20] M. R. Baghbanan, A. Yabuki, R. S. Timsit, and J. K. Spelt, "Tribological behavior of aluminum alloys in a vibratory finishing process," *Wear*, vol. 255, no. 7, pp. 1369–1379, 2003.

[21] A. Yabuki, M. Baghbanan, and J. Spelt, "Contact forces and mechanisms in a vibratory finisher," *Wear*, vol. 252, no. 7, pp. 635–643, 2002.

[22] M. D. Sangid, J. A. Stori, and P. M. Ferriera, "Process characterization of vibrostrengthening and application to fatigue enhancement of aluminum aerospace components:part I. Experimental study of process parameters," *The International Journal of Advanced Manufacturing Technology*, vol. 53, no. 5-8, pp. 545–560, 2011.

[23] D. Ciampini, M. Papini, and J. Spelt, "Characterization of vibratory finishing using the Almen system," *Wear*, vol. 264, no. 7, pp. 671–678, 2008.

[24] D. H. Gane, H. Rumyantsev, B. Diep, and L. Bakow, "Evaluation of vibrostrengthening for fatigue enhancement of titanium structural components on commercial aircraft," in

Ti-2003 Science and Technology, Proceedings of the 10th World Conference on Titanium, Hamburg, Germany, 2003, pp. 1053–1058.

[25] M. D. Sangid, J. A. Stori, and P. M. Ferriera, "Process characterization of vibrostrengthening and application to fatigue enhancement of aluminum aerospace components:part II: Process visualization and modeling," *The International Journal of Advanced Manufacturing Technology*, vol. 53, no. 5-8, pp. 561–575, 2011.

[26] E. Uhlmann, A. Dethlefs, and A. Eulitz, "Investigation into a geometry-based model for surface roughness prediction in vibratory finishing processes," *The International Journal of Advanced Manufacturing Technology*, vol. 75, no. 5-8, pp. 815–823, 2014.

[27] E. Uhlmann, A. Eulitz, and A. Dethlefs, "Discrete element modelling of drag finishing," *Procedia Cirp*, vol. 31, pp. 369–374, 2015.

[28] W.-F. Wang, "Effect of MnS powder additions and vibratory ball peening on corrosion resistance of sintered 316LSC stainless steels," *Powder metallurgy*, vol. 48, no. 2, pp. 151–155, 2005.

[29] D. Ciampini, M. Papini, and J. Spelt, "Modeling the development of Almen strip curvature in vibratory finishing," *journal of materials processing technology*, vol. 209, no. 6, pp. 2923–2939, 2009.

[30] F. Hashimoto and D. DeBra, "Modelling and optimization of vibratory finishing process," *CIRP Annals-Manufacturing Technology*, vol. 45, no. 1, pp. 303–306, 1996.

[31] J. Domblesky, V. Cariapa, and R. Evans, "Investigation of vibratory bowl finishing," *International journal of production research*, vol. 41, no. 16, pp. 3943–3953, 2003.

[32] K. Walton, L. Blunt, and L. Fleming, "The topographic development and areal parametric characterization of a stratified surface polished by mass finishing," *Surface Topography: Metrology and Properties*, vol. 3, no. 3, p. 035003, 2015.

[33] S. Wang, R. Timsit, and J. Spelt, "Experimental investigation of vibratory finishing of aluminum," *Wear*, vol. 243, no. 1, pp. 147–156, 2000.

[34] D. Ciampini, M. Papini, and J. Spelt, "Impact velocity measurement of media in a vibratory finisher," *Journal of materials processing technology*, vol. 183, no. 2, pp. 347–357, 2007.

[35] E. Segurado and F. J. Belzunce, "The Use of Double Surface Treatments to Optimize the Fatigue Life of Components Made on Structural Steels," *Procedia Engineering*, vol. 160, pp. 239–245, 2016.

[36] N. Kawagoishi, T. Nagano, M. Moriyama, and E. Kondo, "Improvement of fatigue strength of maraging steel by shot peening," *Materials and Manufacturing Processes*, vol. 24, no. 12, pp. 1431–1435, 2009.

[37] J. Domblesky, R. Evans, and V. Cariapa, "Material removal model for vibratory finishing," *International Journal of Production Research*, vol. 42, no. 5, pp. 1029–1041, 2004.

[38] A. Mohajerani and J. Spelt, "Edge rounding of brittle materials by low velocity erosive wear," *Wear*, vol. 267, no. 9, pp. 1625–1633, 2009.

[39] SAE, "Titanium alloy, sheet, strip, and plate 6Al–4V annealed," *AMS 4911L: Aerospace Material Specification*, 2007.

[40] A. et Duval, "Acier FADH 14NiCrMo13-4," unknown year.

[41] SAE International, "Computer Generated Shot Peening Saturation Curves, J2597," 2017.

[42] D. Kirk, "Saturation curve analysis and quality control," *Shot Peener*, vol. 20, no. 3, p. 24, 2006.

APPENDIX A   MEASUREMENT METHODS FOR HARDNESS AND RESIDUAL STRESSES

Hardness measurements

Hardness measurements have been performed on the Ti-6Al-4V and E-16NiCrMo13 samples. The surface hardnesses have been measured after polishing manually the samples surface. The in-depth measurements have been realized on the samples cross-section after cutting and polishing (mirror-like). The measurements have been realized at Polytechnique for VP samples and at Safran for SP samples.

A summary of the cutting procedure is presented in Table A.1 for both materials. Table A.2 presents the polishing routine for both materials for all the cross-sections that have been polished. For other surfaces, the polishing routine is the similar but the application force is unknown as the polishing is manual.

The microhardness indentation forces have been calibrated for both materials. Figures A.1a and A.1b present the hardness measurements depending on the indentation force. These indentations forces chosen for Ti-6Al-4V and E-16NiCrMo13 are respectively 100 gf and 300 gf. These forces forces were chosen so that the hardness measurements stabilized and and yielded low scatter.

The microhardness indentation machine has been calibrated on two test blocks that have a hardness of 100 HV (for 100 gf force) and 425 HV (for 300 gf force).

Residual stress measurements

The residual stress measurements have been performed either by StressTech for VP samples or by Safran for SP samples. They both used the DRX method with Moore and Evans' correction method for in-depth measurements. The in-depth measurements were realized by

Table A.1 Cutting of Ti-6Al-4V and E-16NiCrMo13 samples for hardness measurements

Material	Cutting machine	Cutting disk	Rotation speed (rpm)
Ti-6Al-4V	Discotom-10 (Struers)	Cw10-Ti10 (Anamet)	2850
E-16NiCrMo13	Discotom-10 (Struers)	60A25 (Struers)	2850

Table A.2 Polishing routine for microhardness indentation of Ti-6Al-4V and E-16NiCrMo13

Grit	Time	Rotation speed (rpm)	Force (lbs)	Rotation direction (/base)	Additional info
240	3	250	9	Contrary	-
400	3	250	9	Contrary	-
600	3	250	9	Contrary	-
800	3	250	9	Contrary	-
1200	3	250	9	Contrary	-
6 μm	3	250	9	Same	4 drops/30s
3μm	3	250	9	Same	4drops/30s
1μm	3	250	9	Same	4 drops/30s

(a) Calibration of force indentation, Ti-6Al-4V

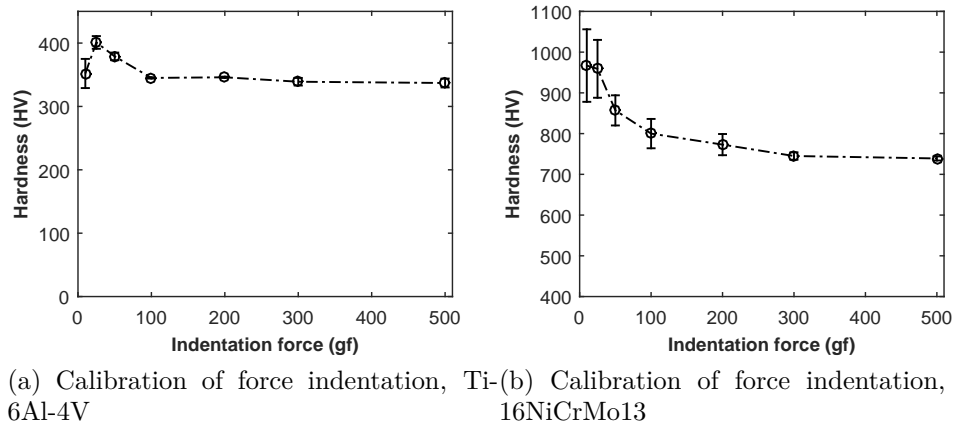(b) Calibration of force indentation, E-16NiCrMo13

Figure A.1 Calibration curves of force indentation for both materials

electropolishing the samples.

StressTech realized the samples electropolishing on a 6.5 mm diameter section using a salted solution and an intensity of 1 A.

The solution composition was:

- 52% salt solution (320-340 g/L NaCl in water, 90-95% saturation)

- 22% EthleneGlycol (Automotive antifreeze)

- 15% Water

- 11% Ethanol (Denatured Alcohol)

The material removal rate was about 1.5 μm per second. Stresstech controlled the depth of the measurements using a Mitutoyo Digital Indicator. The measurements have an expended

accuracy (k=2) of 5.4 μm.

Safran realized the samples electropolishing using a Perchloric acid + alcohol solution. The depth measurements were realized using a Somicronic profilometer.

The calibration of StressTech DRX measurements have been realized on stress free powders, respectively iron and titanium for E-16NiCrMo13 and Ti-6Al-4V samples.